ARTICLE

OBC
www.rsc.org/obc

Chemical models for aspects of the photosynthetic reaction centre: synthesis and photophysical properties of tris- and tetrakis-porphyrins that resemble the arrangement of chromophores in the natural system

Maxwell J. Crossley,*[a] Paul J. Sintic,[a] James A. Hutchison[b] and Kenneth P. Ghiggino*[b]

[a] *School of Chemistry, The University of Sydney, NSW 2006, Australia. E-mail: m.crossley@chem.usyd.edu.au; Fax: 61 2 9351 3329; Tel: 61 2 9351 2751*

[b] *Photophysics Laboratory, School of Chemistry, The University of Melbourne, Victoria, 3010, Australia. E-mail: ghiggino@unimelb.edu.au*

Received 22nd October 2004, Accepted 14th December 2004
First published as an Advance Article on the web 1st February 2005

Tris-porphyrin and tetrakis-porphyrin arrays **1** and **2** are proposed as models for the arrangement of the chromophores that constitute photosynthetic reaction centres (PRC's). Their porphyrinic chromophores are similar in distance apart to the key chromophores of PRC's and the C_2 symmetric arrangement of the macrocycles that constitute the 'special pair' where charge separation occurs is also incorporated. The use of zinc(II) and gold(III) chelation establishes an energy gradient for photoinduced electron transfer across each compound. Synthesis was achieved in good yields through a strategy that used the construction of biquinoxalinyl and Tröger's base linkages between the porphyrinoid components. Compounds which are bis-porphyrin molecular components of the arrays were also synthesised. Photophysical analyses indicate that long-range photoinduced energy and electron transfer processes occur in the extended arrays in addition to those occurring in the component bis-porphyrins. Evidence for step-wise electron transfer between terminal zinc(II)-chelated and gold(III)-chelated porphyrins has been detected in both porphyrins **1** and **2** in polar solvents, representing charge transfer across 35 Å and 50 Å, respectively. At 298 K, in deaerated benzonitrile, the lifetime of the charge transfer state of the tris-porphyrin **1** is 150 ns and the lifetime of the charge transfer state of tetrakis-porphyrin **2** is 59.4 μs; very long when compared to simpler chemical model systems, but still much shorter than the 1 s lifetime of the charge separated state of natural PRC's in cell membranes.

Introduction

Photosynthesis in higher plants, eukaryotic algae and certain bacteria is largely based on porphyrinoid pigments that are assembled in most exquisite architectures.[1] In the photosynthetic reaction centres (PRC's) porphyrinic macrocycles are assembled into arrays where light energy is converted into electrical energy and then into chemical energy in high efficiency. The structure of the PRC's of purple bacteria[2] and Photosystems I and II of the cyanobacterium *Synechococcus elongatus*[3,4] show a very similar arrangement of the porphinoid pigments involved in charge separation despite there being substantial differences in the rest of their photosynthetic apparatus. In particular, different chemical products are produced by the two systems, porphyrinoid macrocycles of a different oxidation level are used within their PRC's (bacteriochlorin in one case and chlorin in the other) and both the number of pigments used and the architecture of their light-harvesting arrays are very different.[1] The fact that the arrangement of the chromophores in PRC's is conserved across the range of natural photosynthetic systems suggests that there is a particular advantage in this motif.

There has been continuing interest in the development of porphyrin arrays in an attempt to model natural electronic processes in which chromophores are separated by conjugated bridges or chemical bonds at either the *meso*- or β-pyrrolic position on the porphyrin macrocycle,[5–11] or which involve supramolecular assemblies.[12,13] Systems have also been designed to create an energy gradient through the incorporation of either quinone or fullerene electron acceptors[14–16] or metal chelation of porphyrin macrocycles,[17–19] enabling the unidirectional transfer of energy or electrons. Photovoltaic and photonic applications of porphyrin arrays have also been investigated.[20–25]

Recently we investigated an approach to model PRC's with porphyrin arrays in which the chromophores are separated by quinoxaline Tröger's base linkers and biquinoxalinyl linkers appended to the porphyrins through β-pyrrolic positions.[10,26] The constituent macrocycles in these systems were shown to be weakly interacting with the linkers mediating energy and electron transfer by a superexchange mechanism. On that basis, we proposed tris-porphyrin **1** as a rationally designed model of the PRC.[10] This system contains a quinoxaline Tröger's base linkage that establishes C_2 symmetry like the charge separation special pair, thereby mimicking an important aspect of the PRC, and a biquinoxalinyl linker. Tris-porphyrin **1** is also an accurate distance model for the PRC with interchromophoric distances that are remarkably similar to those found in nature.[10] In addition the distance between the outer two macrocycles is approximately equal to the distance between the special pair and the final quinone electron acceptor. Selective metallation is expected to significantly alter the excited singlet energy and redox potentials of the terminal chromophores in **1**, allowing directional photoinduced energy and electron transfer processes to occur in the array. Zinc(II) chelated porphyrin has a ~0.15 eV higher excited singlet energy than its free-base analogue and is well known to act as an efficient excitation energy donor to free-base porphyrin.[11] The gold(III) chelated porphyrin is known to be a strong electron acceptor with the site of reduction at the metal centre.[27–29] Thus, array **1** is designed such that after photon absorption at the zinc(II) porphyrin, excitation energy should be transferred efficiently to the free-base porphyrin, where it can initiate an electron transfer to the gold(III) porphyrin. A second electron transfer reaction can also occur, whereby the free-base radical cation is reduced by the zinc(II) porphyrin to form the zinc(II) radical cation. The overall result is the shift of the positive charge initially at the gold(III) porphyrin to the zinc(II) porphyrin, a distance of about 35 Å.

In this paper we also propose the zinc(II)–gold(III) tetrakis-porphyrin **2** as a PRC model and as an extended porphyrin array

DOI: 10.1039/b416204h

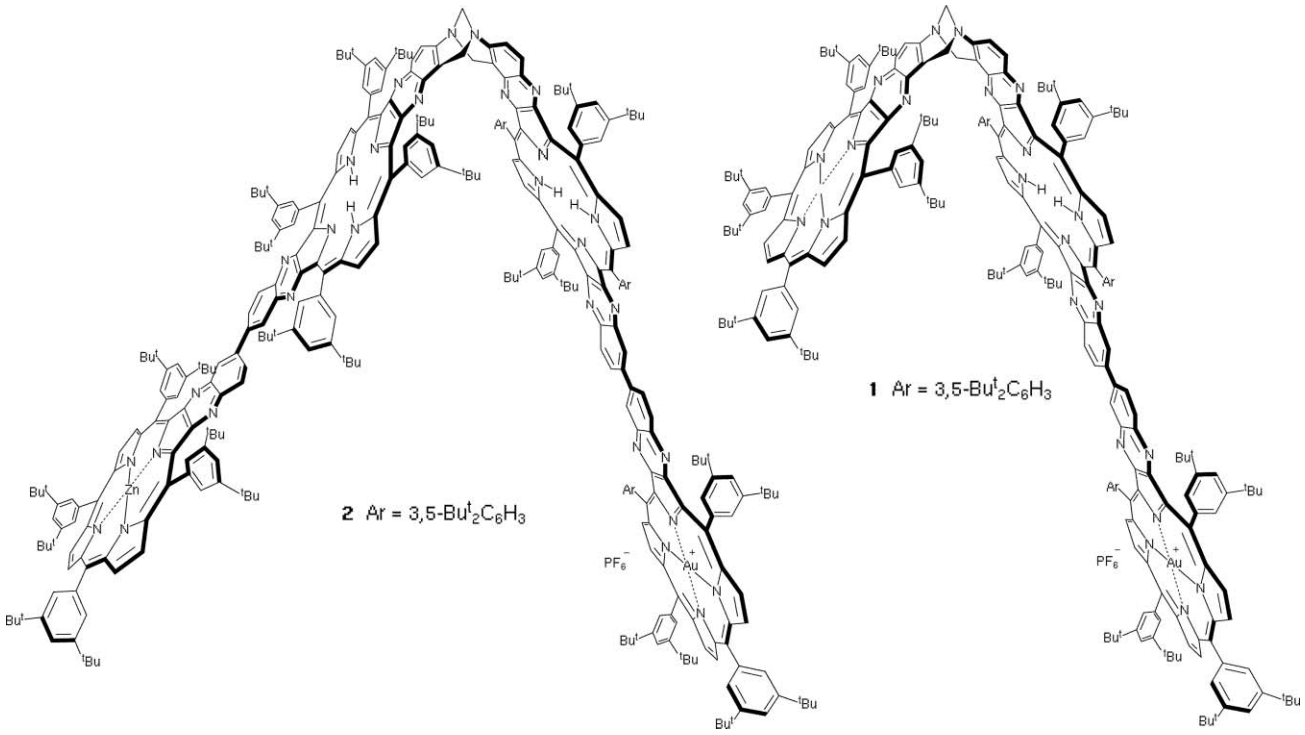

with the ability to exhibit multiple energy and electron transfer processes of interest in the area of molecular electronics.

Tetrakis-porphyrin **2** resembles the arrangement of natural PRC's even more closely than tris-porphyrin **1** in that it has both M- and L-branches.[2] In nature, charge separation at the special pair leads to an electron being conducted along the L-branch to an acceptor, which is either a quinone or iron–sulfur complex, leaving the special pair with a positive charge. In purple bacteria, there is a tightly bound cytochrome unit of four haem groups, situated on the periplasmic side of the biological membrane located near to the special pair, that donates an electron to the special pair to return it to its resting state. In photosystem II this step is achieved by accepting an electron from a nearby tyrosine which is in turn coupled to the manganese complex that produces dioxygen from water. In tetrakis-porphyrin **2**, the terminal Zn(II) porphyrin on the 'M-branch" will act as this electron donor to the special pair pigments; a deviation from nature, but incorporating most of the elements of the photosynthetic charge separation process. Molecular modelling revealed that the interchromophoric separation between terminal zinc(II) and gold(III) macrocycles in **2** is about 50 Å.[30] Photoexcitation of the tetrakis-porphyrin **2** at the zinc(II) porphyrin should result in excitation energy transfer to the adjacent free-base porphyrin, and then between the free-base pair, to initiate an electron transfer to the gold(III) porphyrin. Once again, after the initial charge transfer has occurred the positive charge at the free-base porphyrin may be transferred to the terminal zinc(II) chromophore by successive electron transfer reactions.

In this paper we report the synthesis of zinc(II)-gold(III) tris- and tetrakis-porphyrins **1** and **2** along with model compounds **23**, **26** and **27** that will facilitate photochemical analysis. Preliminary investigations into the photo-induced processes occurring in these molecules is also presented.

Results and discussion

Synthesis of tris- and tetrakis-porphyrins

The synthesis of the zinc(II)-gold(III) tris-porphyrin **1** is outlined in Schemes 1–3. Synthetic precursors were prepared from porphyrin-dione **3** and porphyrin-tetraone **9** (Scheme 1).[31,32] Condensation of **3** with 3,3′-diaminobenzidine **6** (1 eq.) gave diaminobenzidine porphyrin **7** in 78% yield. The formation of the 2 : 1 adduct **8** was avoided by gradually adding porphyrin-dione **3** over 8 h to a dilute solution containing excess **6**. Condensation of **9** with 1,2-diamino-4-nitrobenzene **4** gave 6′-nitroquinoxalino-porphyrin-dione **11** in 42% yield. Likewise, formation of the bis-appended product **10** was minimised by gradually adding 0.5 eq. of **4** to **9** during the reaction. Condensation of **3** and **4** followed by reduction with tin(II) chloride dihydrate and concentrated hydrochloric acid gave 6′-aminoquinoxalino-porphyrin **5** in 66% yield for the two steps.

The condensation of **7** and **11** gave an inseparable regiochemical mixture of *anti*- and *syn*-nitroquinoxalino biquinoxalinyl bis-porphyrins **12** in 94% yield after recrystallisation. (Scheme 2). Regioisomers are obtained as the diaminobenzidine substituent on **7** can condense in a *syn*- or *anti*-orientation relative to the C–C bond of the biquinoxalinyl linker.† The free-base bis-porphyrins **12** were reduced to form the corresponding amino-substituted analogues **14** in 99% yield. Reaction of **12** with potassium tetrachloroaurate(III) gave monogold(III) nitroquinoxalino biquinoxalinyl bis-porphyrins **13** in 20% yield, together with unreacted starting material. The nitro functionality on **13** was then reduced to give monogold(III) aminoquinoxalino biquinoxalinyl bis-porphyrins **15** in 99% yield. The amino bis-porphyrins **14** and **15** were immediately used in the following steps as these compounds readily reacted to form photo-oxidised products in the presence of air and light. The use of **14** and **15** in subsequent steps gave a regiochemical mixture of tris- and tetrakis-porphyrins but their photochemical properties can be considered conjointly since interchromophoric distances are essentially identical.

Multiporphyrin arrays were afforded by the acid-catalysed condensation of monogold(III) aminoquinoxalino biquinoxalinyl bis-porphyrins **15** with 6′-aminoquinoxalino porphyrin **5** (1.5 eq.) and excess formaldehyde (Scheme 3). The mixture was then heated at reflux under nitrogen for 2 days. Excess **5** was added to facilitate the formation of the tris-porphyrin structure,

† For simplicity, only the *anti*-adducts will be depicted in reaction schemes.

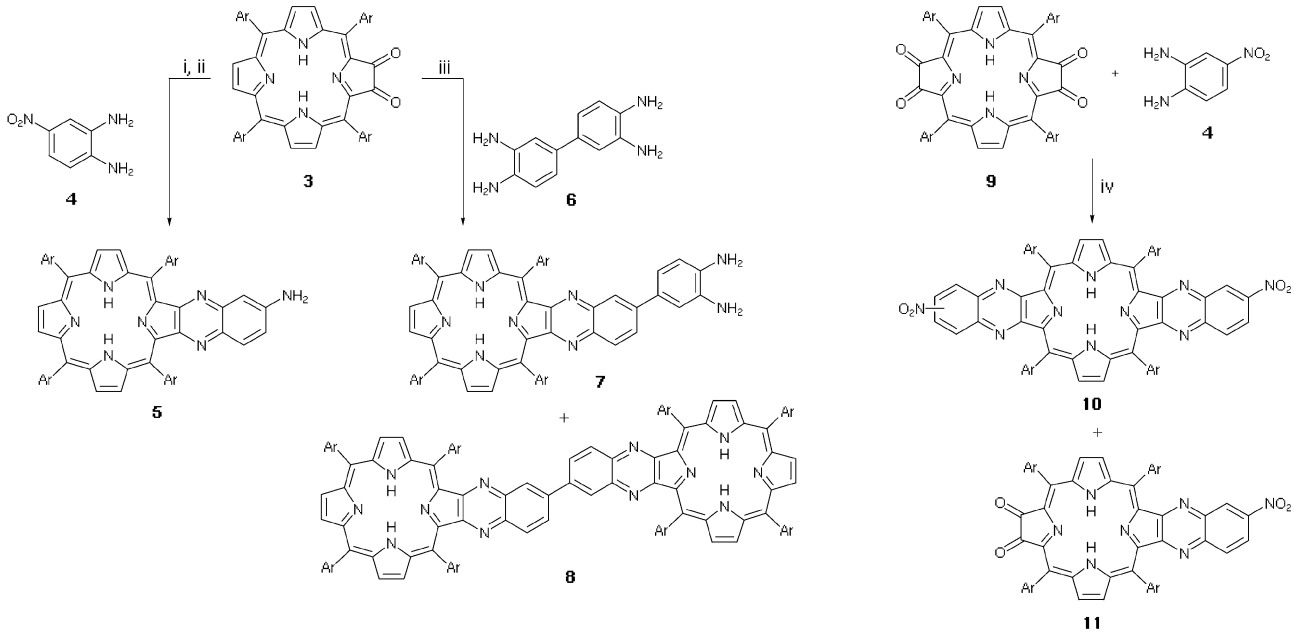

Scheme 1 *Reagents and conditions*: i) CH_2Cl_2, pyridine; ii) $SnCl_2 \bullet 2H_2O$, HCl, CH_2Cl_2; iii) CH_2Cl_2, stir; iv) CH_2Cl_2, pyridine (Ar = 3,5-$Bu^t{}_2C_6H_3$).

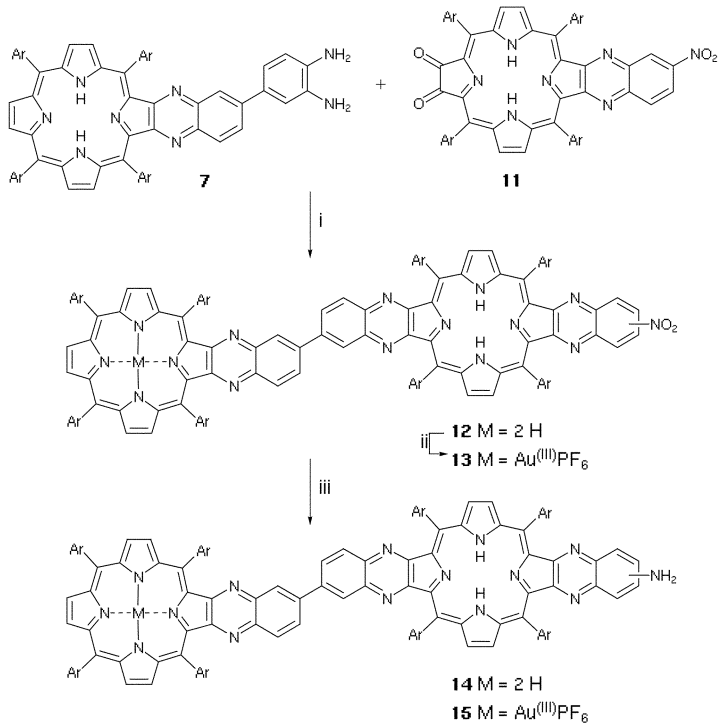

Scheme 2 *Reagents and conditions*: i) $CHCl_3$, stir; ii) $KAuCl_4$, NaOAc, CH_3CO_2H, $CHCl_3$, Δ, 72 h then KPF_6, H_2O, $CHCl_3$, stir 24 h; iii) $SnCl_2 \bullet 2H_2O$, HCl, $CHCl_3$ (Ar = 3,5-$Bu^t{}_2C_6H_3$).

as when equivalent ratios of reactants were added the reaction products were not produced in the expected statistical ratio since the larger molecules took a longer time to react. The reaction products were dissolved in chloroform and methanol and heated at reflux in the presence of zinc(II) acetate for 3 h, followed by ligand exchange with potassium hexafluorophosphate. It was reasoned, correctly as it transpired, that chelation of zinc(II) would preferentially chelate to the chlorin-like core in **1** as opposed to the central bacteriochlorin-like core, that are the result of bond fixation imposed by the fused ring.[32]

The resultant mixture was fractionated by chromatography over silica and three major bands were collected. The first band gave dizinc(II) extended Tröger's base bis-porphyrin **16**, the second band gave zinc(II)–gold(III) tris-porphyrins **1** and the third band gave digold(III) tetrakis-porphyrins **17**. The zinc(II)–gold(III) tris-porphyrins **1** were further purified by size exclusion chromatography to remove decomposed starting material, then reverse phase HPLC to remove traces of dizinc(II) chelated adducts. The zinc(II)–gold(III) tris-porphyrins **1** were obtained in 54% yield. The ^{1}H NMR spectrum (400 MHz) of **1** displayed a singlet at δ 4.45 and two doublet of doublets with geminal coupling of 17.8 Hz at δ 4.54 and 4.80, each signal accounting for two protons and thus indicating the presence of the methano–diazocine bridge in these molecules. The inner NH resonances appeared as two singlets at δ −2.43 and −2.45 indicating that the protons of the free-base bacteriochlorin-like core are in unique chemical environments due to different substituents at the β-pyrrolic positions adjacent to these protons. The MALDI-TOF

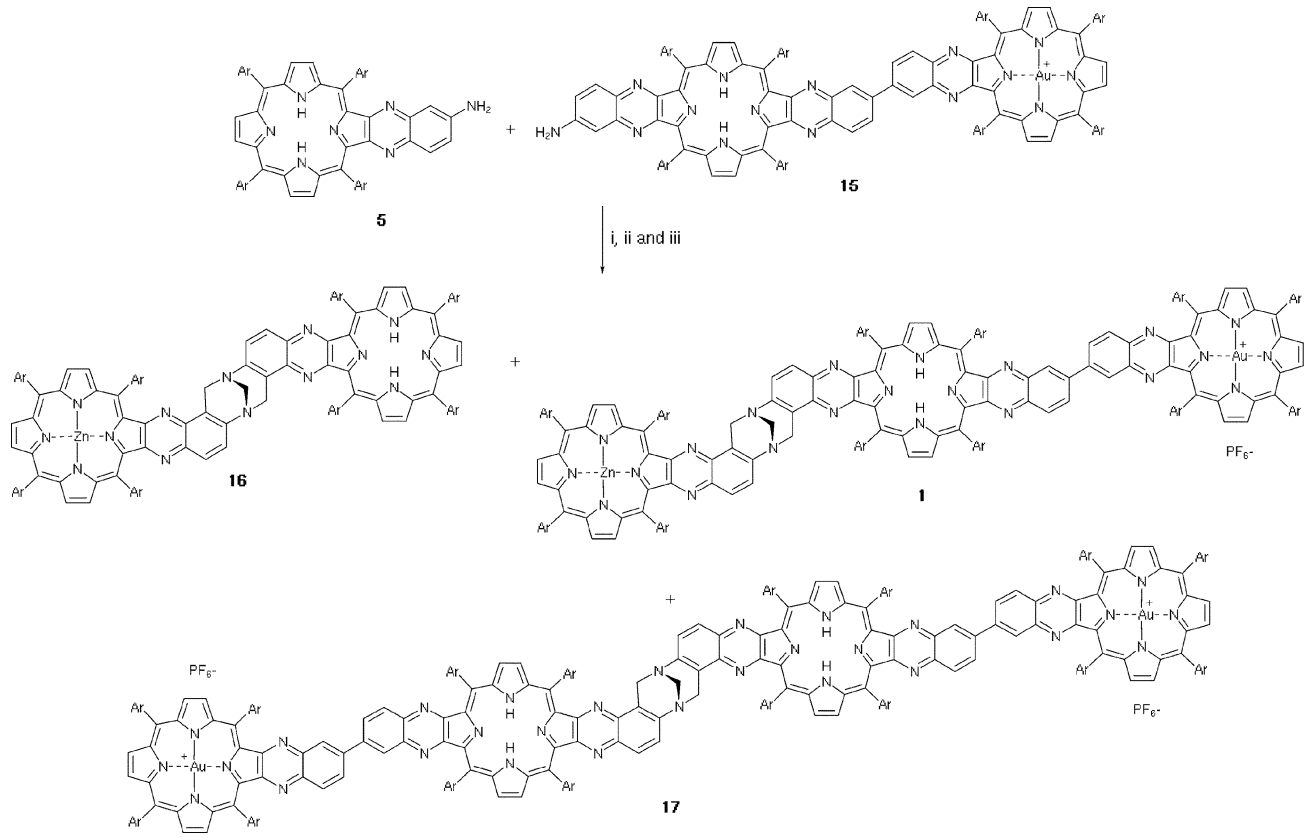

Scheme 3 *Reagents and conditions*: i) HCHO, THF, HCl, Δ, 48 h; ii) $Zn(OAc)_2 \bullet 2H_2O$, $CHCl_3$, Δ; iii) KPF_6, H_2O, $CHCl_3$, stir 24 h (Ar = 3,5-$Bu^t{}_2C_6H_3$).

mass spectrum of **1** was consistent with the molecular formula of $C_{255}H_{286}N_{22}Au$, the PF_6^- counterion being lost in flight.

The zinc(II)–gold(III) tetrakis-porphyrins **2** were prepared by the acid-catalysed condensation of monogold(III) aminoquinoxalino biquinoxalinyl bis-porphyrins **15** with aminoquinoxalino biquinoxalinyl bis-porphyrins **14** (1.5 eq.) in the presence of excess formaldehyde (Scheme 4). The reaction was heated at reflux for 5.5 days under nitrogen to ensure that the reaction went to completion. The reaction product was then dissolved in mixture of chloroform and methanol and treated with zinc(II) acetate dihydrate at room temperature for 6 h, followed by ligand exchange with potassium hexafluorophosphate. The zinc(II) metallation reaction in this synthesis was performed under milder conditions than those used in the corresponding step in the synthesis of tris-porphyrin **1** in order to reduce the likelihood of zinc(II) chelation to the central free-base bacteriochlorin-like cores in the tetrakis-porphyrin structure. This approach was successful as such by-products were not detected.

Fractionation of the reaction mixture by chromatography over silica gave three major bands. Size exclusion chromatography of the product from the second band, to remove bis-porphyrin impurities, gave zinc(II)–gold(III) tetrakis-porphyrins **2** in 42% yield. The first and third bands yielded, respectively, dizinc(II) tetrakis-porphyrins **18** and digold(III) tetrakis-porphyrins **17**.

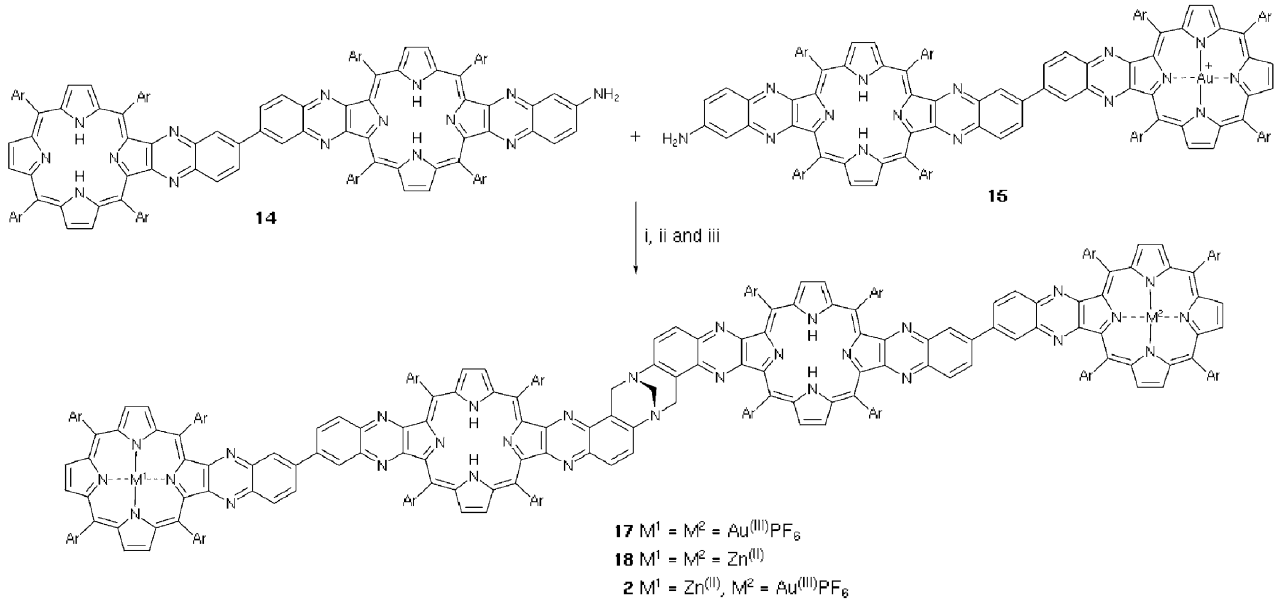

Scheme 4 *Reagents and conditions*: i) HCHO, THF, HCl, Δ, 48 h; ii) $Zn(OAc)_2 \bullet 2H_2O$, $CHCl_3$, Δ; iii) KPF_6, H_2O, $CHCl_3$, stir 24 h (Ar = 3,5-$Bu^t{}_2C_6H_3$).

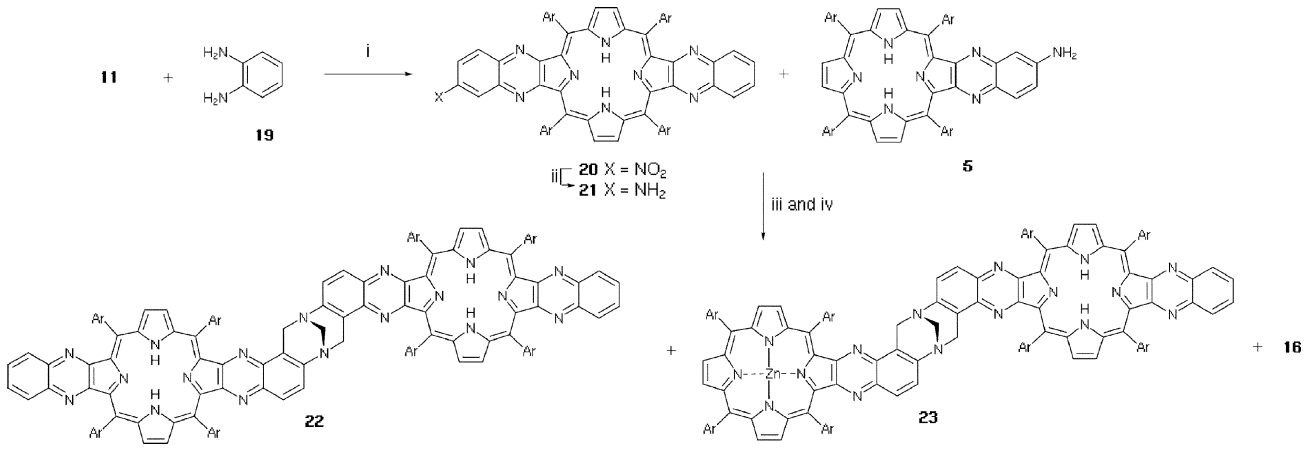

Scheme 5 *Reagents and conditions*: i) $CHCl_3$, stir, 24 h; ii) $SnCl_2 \bullet 2H_2O$, $CHCl_3$, HCl, 3 days; iii) HCHO, THF, HCl, Δ, 48 h; iv) $Zn(OAc)_2 \bullet 2H_2O$, $CHCl_3$, MeOH, room temp., 8 h (Ar = 3,5-Bu$^t_2$C$_6$H$_3$).

The ^{1}H NMR spectrum of **2** confirmed the presence of the methano–diazocine bridge and free-base bacteriochlorin-like cores contained within the molecule. The MALDI-TOF mass spectrum was consistent with the molecular formula of $C_{343}H_{382}N_{22}Au$, the PF_6^- counterion again being lost.

Synthesis of molecular components

The bis-porphyrin model compounds that contain the extended Tröger's base and biquinoxalinyl linkers **23**, **26** and **27** were also required in order to determine the role that the connecting bridges play in mediating energy and electron transfer between chlorin-like and bacteriochlorin-like macrocycles. This information should assist interpretation of the more complex processes that were expected to occur in the photoactive multiporphyrin arrays **1** and **2**.

Monozinc(II) extended Tröger's base quinoxaline-appended bis-porphyrin **23** was prepared by the acid-catalysed condensation of 6′-aminoquinoxalino-porphyrin-quinoxaline **21** (prepared by the condensation between porphyrin-6′-nitroquinoxaline-dione **11** and *o*-phenylenediamine **19**, followed by reduction of the resultant reaction product), 6′-aminoquinoxalino porphyrin **5** and excess formaldehyde, followed by stirring the resultant mixture with zinc(II) acetate dihydrate for 8 h at room temperature (Scheme 5). TLC and MALDI-TOF mass spectrum indicated the generation of the expected three reaction products, although after purification by column chromatography only **23** and **16** were isolated in 16% and 15% yield, respectively. Trace quantities of impure **22** were collected before elution of the first major band during chromatography. This compound appeared to be unstable in air and light and decomposed during chromatography. The ^{1}H NMR spectrum of **23** revealed four one-proton doublets at δ 4.54, 4.55, 4.79 and 4.82, with geminal coupling of 17.6 Hz and a broad singlet, accounting for two protons, at δ 4.45. This confirmed that all the protons of the methano–diazocine bridge are all in unique environments, as expected for an asymmetric molecule. The bacteriochlorin-like macrocycle in **23** was not metallated, as evident by the presence in the ^{1}H NMR spectrum of the inner NH signals as one-proton singlets at δ −2.52 and −2.50. The parent ion in the MALDI-TOF mass spectrum confirmed the molecular formula of $C_{173}H_{196}N_{16}Zn$.

Free-base biquinoxalinyl quinoxaline-appended bis-porphyrin **25** was prepared in 94% yield by the condensation of diaminobenzidine porphyrin **7** and quinoxalino porphyrin-dione **24**. Compound **24** was prepared by the condensation of porphyrin-tetraone **9** and *o*-phenylenediamine **19**.[33] Metallation of **25** with zinc(II) acetate dihydrate gave monozinc(II) biquinoxalinyl quinoxaline-appended bis-porphyrin **26** in

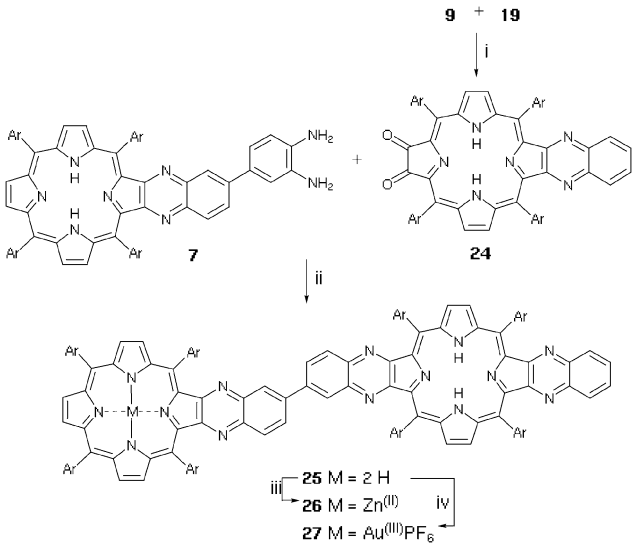

Scheme 6 *Reagents and conditions*: i) CH_2Cl_2–pyridine, stir; ii) $CHCl_3$, stir, 48 h; iii) and iv) see text (Ar = 3,5-Bu$^t_2$C$_6$H$_3$).

99% yield (Scheme 6). Microanalysis was consistent with the molecular formula ($C_{170}H_{190}N_{14}Zn$) of the assigned structure.

Monogold(III) biquinoxalinyl quinoxaline-appended bis-porphyrin **27** was prepared in 21% yield after **25** was dissolved in a solution of acetic acid and chloroform with excess potassium tetrachloroaurate(III) and sodium acetate and heated for 3 days, followed by ligand exchange with hexafluorophosphate (Scheme 6). The MALDI-TOF mass spectrum confirmed the molecular formula of $C_{173}H_{196}N_{16}Au$, the PF_6^- counterion being lost.

The synthesis of monomeric quinoxalino-porphyrin components, zinc(II) and gold(III) quinoxalino-porphyrins **28** and **29** and linear free-base bisquinoxalino-porphyrin **30**, required for the photophysical characterisation of individual chromophoric components in the bis-, tris- and tetrakis-porphyrin arrays, are reported elsewhere.[10,33]

Free-base tris- and tetrakis-porphyrins, **31** and **32**, analogues of **1** and **2**, were obtained as products of the same experiment by reaction of free-base bis-porphyrin **14**, 6′-aminoquinoxalino porphyrin **5** (1.0 eq.) and excess formaldehyde (Scheme 7). The reaction products were separated by size exclusion chromatography, which afforded free-base tris-porphyrins **31** and tetrakis-porphyrins **32** in yields of 21% and 15%, respectively, and extended Tröger's base bis-porphyrin **33** (44%). Microanalysis and the MALDI-TOF mass spectrum confirmed the molecular formulas of tris- and tetrakis-porphyrins, **31** and **32**, as $C_{255}H_{290}N_{22}$ and $C_{343}H_{386}N_{30}$, respectively.

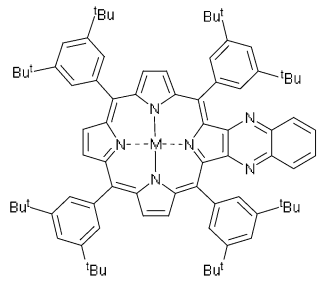

28 M = $Zn^{(II)}$
29 M = $Au^{(III)}PF_6$

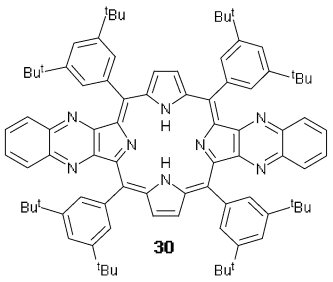

30

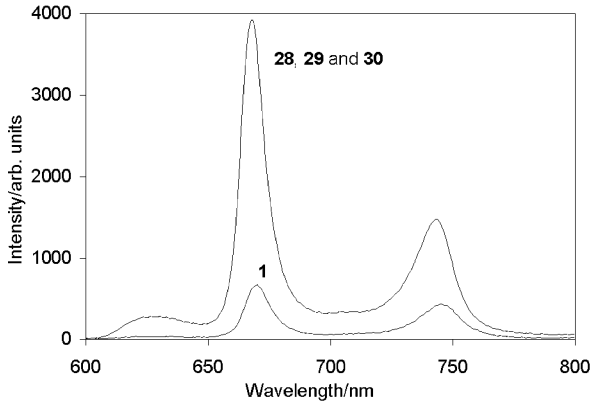

Fig. 1 Corrected fluorescence spectra of the tris-porphyrin **1** and an optically matched, equimolar mixture of monomers **28**, **29** and **30**. Excitation is at 553 nm in aerated THF.

Photophysical studies

Steady-state and time-resolved fluorescence studies of **1** and **2** indicate that photoexcitation of the terminal zinc(II) chromophore initiates energy transfer processes, which in turn drive an electron transfer process from free-base to the gold(III) chromophore at the opposite end of the array.

Fig. 1 shows the fluorescence emission spectrum of the tris-porphyrin array **1** compared with an optically matched, equimolar mixture of its component monomers (excitation is at 553 nm, exciting all chromophores). The fluorescence peak at 629 nm is associated with emission from the zinc(II) chelated chromophore, while the peaks at 668 nm and 744 nm are associated with the free-base chromophore (the gold(III) porphyrin is non-fluorescent). Emission from both the zinc(II) and free-base chromophores is strongly quenched indicating that additional non-radiative deactivation pathways occur in **1** to deactivate the excited states of these chromophores. Strong quenching of zinc(II) and free-base porphyrin fluorescence is also observed in the tetrakis-porphyrin array **2**.

The bis-porphyrins **23** and **26** are suitable models to study the photoinduced interactions between zinc(II) porphyrin and the adjacent free-base porphyrin chromophore in **1** and **2** respectively. Photoexcitation of the bis-porphyrins at the zinc(II) chromophore results in quenching of zinc(II) chromophore fluorescence, with a concomitant enhancement of the free-base porpyhrin fluorescence. This suggests energy transfer from photoexcited zinc(II) to free-base porphyrin is occurring in **23** and **26**, as has been observed previously for a zinc(II)-free-base porphyrin dimer attached across a Tröger's base bridge.[11] Energy transfer from the photo-excited zinc(II) porphyrin in **1** and **2** is confirmed by fluorescence excitation spectra which clearly show free-base porphyrin emission results from excitation at the zinc(II) porphyrin absorption bands. Time-resolved fluorescence studies of the quenched emission suggest energy transfer rates of $\sim 10^{10}$ s^{-1} in a range of solvents for **1** and **2**.

After the initial energy transfer from the zinc(II) chromophore to the neighbouring free-base chromophore in **2**, excitation energy can be transferred between the adjacent free-base chromophores. Energy transfer between like free-base chromophores separated across a Tröger's base bridge was previously measured to occur at a rate of 9.5×10^7 s^{-1} in CH_2Cl_2.[11] In the case of **2** the free-base porphyrin adjacent to the gold(III) porphyrin is quenched by an electron transfer process that is between 15 and 70 times more efficient (*vide infra*). Therefore the energy transfer between free-base moieties is essentially unidirectional.

Bis-porphyrin **27** models the interaction between neighbouring free-base and gold(III) chromophores in **1** and **2**. Free-base

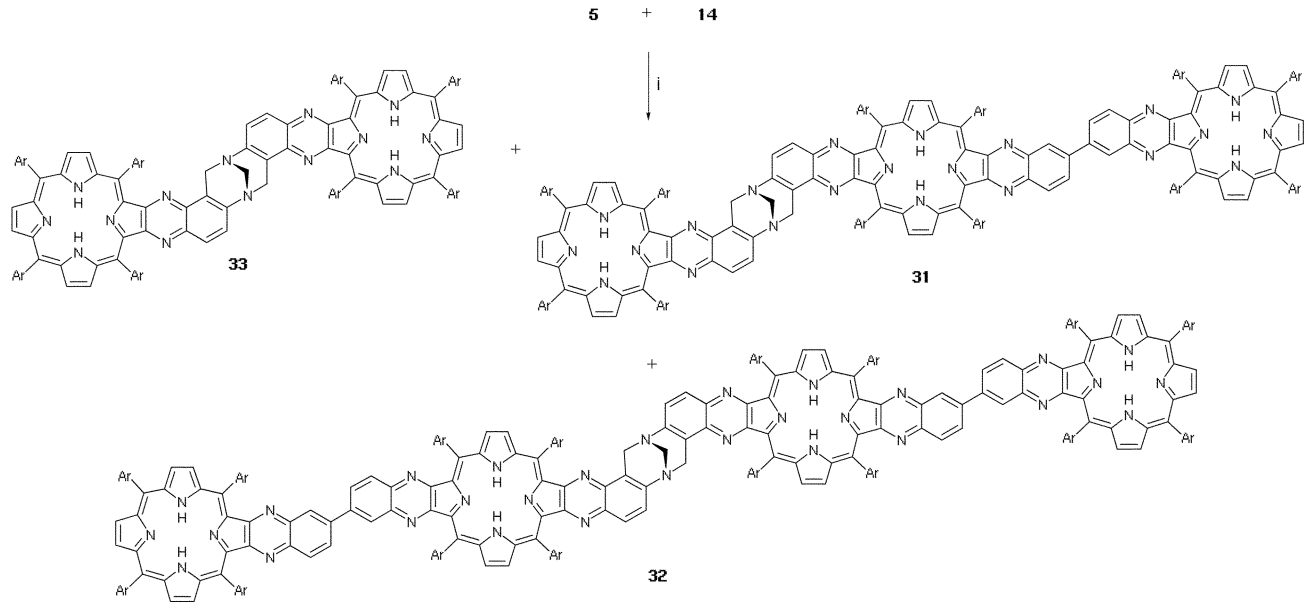

Scheme 7 *Reagents and conditions*: i) HCHO, THF, HCl, Δ, 48 h.

porphyrin emission is >98% quenched for **27** compared to the relevant monomer reference. Previous studies found that photoinduced electron transfer is the dominant quenching mechanism for a photo-excited free-base porphyrin connected to a gold(III) porphyrin by a biquinoxalinyl bridge (energy transfer is precluded as the excited singlet energy of the free-base porphyrin is lower than that of the gold(III) porphyrin).[11,34] For **27**, the free energy change for the photoinduced electron transfer (ΔG°_{CT}) was calculated to be −0.51 eV in THF and is expected to be relatively solvent independent. This is due in part to the electron transfer being a charge shift, in which the positive charge on the gold(III) porphyrin is shifted to the free-base porphyrin, rather than a charge separation in which positive and negative charges are created from a neutral species. Thus solvent dependent coulombic stabilisation can be neglected in the calculation of ΔG°_{CT}.[34] Time-resolved fluorescence studies yielded electron transfer rates that are only mildly solvent dependent, ranging from 1.7×10^9 s^{-1} to 6.9×10^9 s^{-1} for **27** going from toluene to benzonitrile.

Transient absorption spectra of **27**, **1** and **2** were recorded using the laser photolysis technique, with excitation at 541 nm to favour free-base porphyrin absorption. The transient absorption spectra of **1** and **2** in non-polar solvents such as toluene and cyclohexane are similar to that of **27**, indicating no further reactions occur after the initial free-base to gold(III) porphyrin electron transfer. Laser photolysis of **1** and **2** in THF and more polar solvents, however, reveals transient absorption spectra which strongly resemble reported spectra of charge transfer states in zinc(II)/gold(III) porphyrin dimers (Fig. 2).[29]

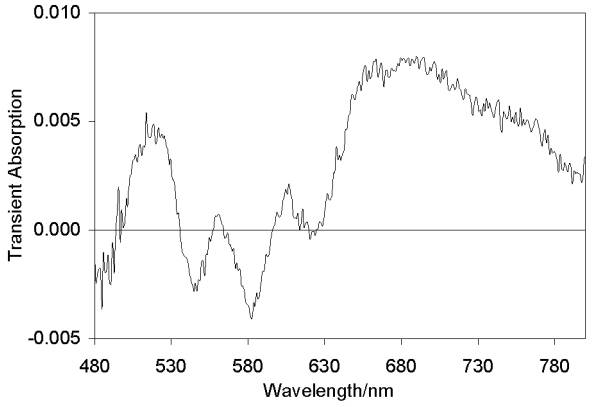

Fig. 2 Transient absorption spectrum of tetrakis-porphyrin **2** recorded in deaerated benzonitrile 10 μs after pulsed excitation at 541 nm (2 ns gate width).

The strong transient absorption in the near infra-red region (650–800 nm) and the bleaching of the zinc(II) porphyrin ground state absorption bands, at 580 and 623 nm, is characteristic of zinc(II) porphyrin radical cation formation, whereas the absence of the free-base porphyrin ground state bleaching at 670 nm indicates that free-base porphyrin is in the ground state in the transient. The transient spectra of **1** and **2** in polar solvents are attributed to a giant charge shifted state in which the zinc(II) porphyrin has been oxidised to the zinc(II) radical cation and the gold(III) porphyrin reduced to the gold(II) porphyrin. The giant charge shifted state is formed within the temporal width of the laser pulse (8 ns) and decays exponentially with a lifetime of 150 ns and 59.4 μs for **1** and **2**, respectively, in deaerated benzonitrile (a minor (<15%) component decaying over milliseconds is also detected and is attributed to porphyrin triplet state formation). As it can be produced by selective excitation of the free-base chromophore, the giant charge shifted state is most likely formed by step-wise reduction of the free-base radical cation (the product of the primary free-base to gold(III) porphyrin charge transfer) until the positive charge resides on the zinc(II) chromophore. Direct electron transfer between zinc(II) and gold(III) porphyrins, with the intervening free-base chromophore(s) acting as a super-exchange medium, may also occur. Further work is under way to fully resolve the mechanism and quantum yields of electron transfer processes in the extended arrays.

Conclusions

Quinoxaline Tröger's base and biquinoxalinyl linkers have been used to build up extended porphyrin arrays, linked through the β-pyrrolic position of the porphyrin macrocycle. The extended porphyrin arrays are good structural homologues to the chromophores of the PRC's and display a similar ability to undergo directional multi-step energy and electron transfer processes upon photoexcitation. Arrays **1** and **2** contain an energy gradient such that photon absorption at the zinc(II) chromophore will initiate an electron transfer to the gold(III) chromophore at the opposite end of the array by rapid transfer of excitation energy. In polar solvents the electron transfer from free-base to gold(III) porphyrin is the primary step in the formation of a long-lived, giant charge shifted state, in which a positive charge is shifted from the gold(III) porphyrin to the zinc(II) porphyrin at the other end of the array. In the tetrakis-porphyrin **2**, this represents charge transfer over a distance of 50 Å. The vectorial transfer of electrons and excitation energy over long distances displayed by arrays **1** and **2** is potentially useful in the creation of molecular devices such as molecular wires and *trans*-membrane pumps. The arrays meet the further requirements of a molecular wire in that the metallated terminal chromophores are redox active and allow the arrays to be 'anchored' to other molecular components.[5,35,36] The geometry of the arrays, with hydrophobic free-base chromophores located centrally between the more hydrophilic terminal metallated porphyrins should encourage the arrays to span across lipid bilayers, thereby mimicking another important feature of natural PRC's which a biological membrane.

As good as they are as distance and orientation mimics, the chemical models of the PRC's presented here have several deficiencies. The first is derived from the use of biquinoxalinyl linkages which produces regioisomers in its formation and which also allows too much conformational freedom within the molecules. This linker also places the 'special pair' porphyrins too far apart and thereby probably unable to delocalise the cation-radical character that these chromophores share in natural PRC's. Another deficiency is that magnesium(II) and free-base partially reduced porphyrins are used in natural systems unlike the zinc(II) and gold(III) porphyrins used in this study. The model compounds **1** and **2** lack an electron acceptor to mimic the quinones and iron–sulfur complexes of natural systems. The models use the gold(III) porphyrin as the electron acceptor and this causes the system to produce a charge shift state rather than a charge separated state, although the charge separated state is achieved in the short-lived intermediates. Work in progress in our laboratory to mimic the PRC's involves the synthesis of compounds in which these deficiencies are overcome.

Experimental

General procedures

Melting points were recorded on a Reichert melting point stage and are uncorrected. Microanalyses were performed by the Campbell Microanalytical Laboratory, University of Otago, New Zealand. Infra-red spectra were recorded on a Perkin-Elmer Model 1600 FT-IR spectrophotometer as solutions in the stated solvents. Intensity abbreviations used are: w, weak; m, medium; s, strong. Ultraviolet-visible spectra were routinely recorded on a Cary 5E UV-Vis-NIR spectrophotometer in chloroform that was deacidified by filtration through an alumina column.

^{1}H NMR spectra were recorded on either a Bruker WM-400 (400 MHz) or AMX-400 (400 MHz) spectrometer as stated. ^{1}H NMR chemical shifts are referenced to internal solvent resonances. ^{31}P NMR spectra were acquired on a Bruker DPX-400 (162 MHz) spectrometer. ^{31}P NMR chemical shifts are referenced to external, neat trimethyl phosphite taken to be 140.85 ppm at room temperature. Deuterated solvents were used as received except for deuterated chloroform, which was deacidified by filtration through a plug of alumina and potassium carbonate. Signals are recorded in terms of chemical shift (in ppm), multiplicity, coupling constants (in Hz) and assignments, in that order. The following abbreviations for multiplicity are used: s, singlet; d, doublet; t, triplet; m, multiplet; h, heptet; dd, doublet of doublets; br, broad; ABq, AB quartet. The porphyrin macrocycles in NMR assignments are denoted as: ZnP, zinc(II) porphyrin; FbP, free-base porphyrin; AuP, gold(III) porphyrin.

Matrix assisted laser desorption ionisation time of flight (MALDI-TOF) mass spectra were recorded without a matrix on a VG TofSpec spectrometer. Mass spectra were obtained as an envelope of the isotope peaks of the molecular ion. The mass corresponding to the envelope's maxima is reported and was compared with the maxima and shape of a simulated spectrum. Fast atom bombardment high resolution mass spectra (FAB-HRMS) were recorded on a VG ZAB-2SEQ instrument at the Research School of Chemistry, Australian National University.

Column chromatography was routinely carried out using the gravity feed column technique on Merck silica gel Type 9385 (230–400 mesh). Analytical thin layer chromatography (TLC) was performed on Merck silica 60 F_{254} precoated sheets (0.2 mm) in the stated solvents. Size-exclusion chromatography was conducted using a gravity feed column (3 cm ID × 120 cm) containing Biobeads (S-X1 polystyrene based size-exclusion particles) using toluene as the eluent (flow rate 0.5 cm^3 min^{-1}).

Analytical high performance liquid chromatography (HPLC) was performed with a Waters 600E multisolvent pump, Rheodyne 7725i injector and a Waters 486 tunable absorbance multiwavelength detector (set at 420 nm) controlled by Millennium software. An Altech Altima C18 (4.6 mm ID × 25 cm, 5 μm particle size) column was used at an elution rate of 1 cm^3 min^{-1} in the stated solvent system. Preparative HPLC was performed with a Waters 600E multisolvent pump, Rheodyne 7725i injector and a Waters 486 tunable absorbance multiwavelength detector (set at 420 and 520 nm) controlled by Millennium software. The column used was Altech Altima C18 (22 mm ID × 30 cm, 10 μm particle size) eluting at a rate of 7 cm^3 min^{-1} in the stated solvent system.

All solvents used were redistilled before use, unless otherwise stated. Light petroleum refers to the fraction of bp 60–80 °C. Chloroform was distilled from potassium carbonate prior to use as a HPLC solvent. Where solvent mixtures were used, the proportions are given by volume.

Electrochemistry was performed using a BAS 100 Electrochemical Analyser. All measurements were made at room temperature, on samples dissolved in distilled dichloromethane or freshly distilled tetrahydrofuran, with electrochemical grade 0.1 M tetrabutylammonium perchlorate (TBAP) as the supporting electrolyte. A glassy carbon working electrode, platinum wire auxiliary electrode and a Ag–AgCl–KCl (sat.) reference electrode were used. The solutions were de-oxygenated by saturation with oxygen-free argon. The tetrahydrofuran was purified in two steps; firstly, it was dried over sodium wire, and secondly, distilled over sodium wire and benzophenone under nitrogen. The scan rate used in all cyclic voltammetry (CV) experiments was 100 mV s^{-1}.

Steady state fluorescence measurements were carried out using a Varian Cary Eclipse fluorescence spectrophotometer. Time-resolved fluorescence measurements were carried out using the time-correlated single photon counting technique, the details of the apparatus have been published elsewhere.[37] Samples were prepared in 1 cm pathlength cells using spectroscopic grade solvents and were deaerated by repeated freeze–pump–thaw cycles. Sample absorbance at the excitation wavelength was kept below 0.2 to avoid reabsorption and inner filter effects.

Transient absorption measurements were carried out using the laser photolysis technique. The excitation source was a tunable OPO (Cassix BBO-3B/SHG) pumped by a Nd:YAG laser (Continuum NY-61, 8 ns pulse width, 3 mJ per pulse). Sample absorption was less than 0.6 at the excitation wavelengths. Solutions were probed at right angles to excitation with a Xe arc lamp (Rofin) and the probe light focussed through a spectrograph (Acton SpectraPro 300i). Transient spectra were recorded on a gated, intensified CCD camera (Princeton Instruments ICCD-MAX). Transient decays were recorded using a photomultiplier tube (Hamamatsu R928) and digital oscilloscope (Tektronix TDS-520).

5,10,15,20-Tetrakis(3,5-di-*tert*-butylphenyl)-6′-(3″,4″-diaminophenyl)quinoxalino[2,3-*b*]porphyrin 7. 2,3-Dioxo-5,10,15,20-tetrakis(3,5-di-*tert*-butylphenyl)chlorin **3** (940 mg, 0.86 mmol) was added over 4 h to a stirring solution of 3,3′-diaminobenzidine **6** (540 mg, 2.52 mmol) in dichloromethane (700 cm^3). The mixture was then stirred for an additional 3 h with the reaction being monitored by TLC analysis. When the reaction had gone to completion the solvent was removed under a vacuum and the residue purified by chromatography over silica (dichloromethane–light petroleum; 1 : 1 changing to dichloromethane–methanol; 100 : 3). The front running band was collected and the solvent removed to afford bis-6′,6′-{5,10,15,20-tetrakis(3,5-di-*tert*-butylphenyl)quinoxalino[2,3-*b*]-porphyrin} **8** (65 mg, 6.5%) as a green microcrystalline solid, mp >300 °C, which co-chromatographed and had an identical ^{1}H NMR spectrum to an authentic sample.[10]

The major polar band was collected, the solvent evaporated to dryness and the residue recrystallised from a mixture of dichloromethane-methanol to afford 5,10,15,20-tetrakis(3,5-di-*tert*-butylphenyl)-6′-(3″,4″-diaminophenyl)quinoxalino[2,3-b]porphyrin **7** (850 mg, 78%) as purple crystals, mp >300 °C (FAB-HRMS found: M$^+$ 1270.8227. $C_{88}H_{102}N_8$ requires 1270.8227); $\nu_{max}(CHCl_3)$/cm^{-1} 3458s, 2965s, 2078w, 1709m, 1636m, 1593m, 1477m, 1364m and 1248m; $\lambda_{max}(CH_2Cl_2)$/nm 437 (log ε 5.35), 531 (4.39), 565 (3.86), 600 (4.12) and 652 (3.09); δ_H(400 MHz; $CDCl_3$) −2.51 (2 H, s, inner NH), 1.57 (15 H, s, *t*-butyl H), 1.59 (15 H, s, *t*-butyl H), 1.64 (42 H, s, *t*-butyl H), 3.45–4.05 (4 H, br s, NH_2), 6.97 (1 H, d, $J_{2'',1''}$ 7.8, H-2″), 7.22 (1 H, d, $J_{5'',1''}$ 1.9, H-5″), 7.24 (1 H, dd, $J_{1'',2''}$7.8, $J_{1'',5''}$1.9, H-1″), 7.89 (3 H, m, aryl H and H-5′ or H-13′ or H-14′), 8.02 (2 H, m, aryl H), 8.04 (1 H, br s, H-5′ or H-13′ or H-14′), 8.06 (2 H, d, *J* 1.8, aryl H), 8.07 (2 H, d, *J* 1.8, aryl H), 8.19 (5 H, m, aryl H and H-5′ or H-13′ or H-14′), 8.87 (2 H, s, β-pyrrolic H), 9.07 and 9.15 (4 H, ABq, J_{AB} 4.7, β-pyrrolic H); *m*/*z* (MALDI-TOF) 1271.8 (M$^+$ requires 1271.8).

5,10,15,20-Tetrakis(3,5-di-*tert*-butylphenyl)-6′-aminoquinoxalino[2,3-*b*]porphyrin 5. 2,3-Dioxo-5,10,15,20-tetrakis(3,5-di-*tert*-butylphenyl)chlorin **3** (360 mg, 0.329 mmol) and 1,2-diamino-4-nitrobenzene **4** (103 mg, 0.673 mmol) were dissolved in a solution of dichloromethane (25 cm^3) and pyridine (3 cm^3) and stirred for 4 days. The solvent was removed under a vacuum and the residue purified by chromatography over silica (dichloromethane–light petroleum; 1 : 1). The major band was collected and the solvent evaporated to dryness to yield 5,10,15,20-tetrakis(3,5-di-*tert*-butylphenyl)-6′-nitroquinoxalino[2,3-*b*]porphyrin (308 mg) as a reddish–purple microcrystalline solid, mp >300 °C, which co-chromatographed and had identical spectroscopic data to an authetic sample.[26] 5,10,15,20-tetrakis(3,5-di-*tert*-butylphenyl)-6′-nitroquinoxalino[2,3-*b*]porphyrin and tin(II) chloride dihydrate (308 mg, 0.253 mmol) were dissolved in dichloromethane (40 cm^3). Hydrochloric acid (10 M, 1 cm^3) was then added and the mixture stirred in the dark for 5 days under nitrogen. The mixture was then diluted with

dichloromethane (200 cm^3) and washed with water (200 cm^3), sodium carbonate solution (10%, 2 × 200 cm^3) and water (2 × 200 cm^3), dried over anhydrous sodium sulfate and filtered. The filtrate was evaporated to dryness and the residue purified by chromatography over silica (dichloromethane–light petroleum; 1 : 1). The major band was collected, the solvent removed and the residue recrystallised from a dichloromethane–methanol solution to afford 5,10,15,20-tetrakis(3,5-di-*tert*-butylphenyl)-6′-aminoquinoxalino[2,3-*b*]porphyrin **5** (255 mg, 66%) as a dark brown microcrystalline solid, mp >300 °C, which co-chromatographed and had an identical ^{1}H NMR spectrum to an authentic sample.[26] δ_H(400 MHz; $CDCl_3$) −2.48 (2 H, br s, inner NH), 1.49–1.53 (72 H, m, *t*-butyl H), 4.12 (2 H, br s, NH_2), 6.88 (1 H, d, $J_{5',7'}$ 2.3, H-5′), 7.17 (1 H, dd, $J_{7',8'}$ 8.9, $J_{7',5'}$ 2.3, H-7′), 7.60 (1 H, d, $J_{8',7'}$ 8.9, H-8′), 7.80 (2 H, t, *J* 1.5, aryl H), 7.90 (2 H, br s, aryl H), 7.97 (4 H, d, *J* 1.6, aryl H), 8.10 (4 H, d, *J* 1.6, aryl H), 8.80 (2 H, s, β-pyrrolic H), 8.97 and 9.02 (2 H, ABq, J_{AB} 4.6, β-pyrrolic H), 8.98 and 9.05 (2 H, ABq, J_{AB} 4.6, β-pyrrolic H); *m*/*z* (MALDI-TOF) 1181.0 (M^+ requires 1180.7).

12,13-Dioxo-5,10,15,20-tetrakis(3,5-di-*tert*-butylphenyl)-6′-nitroquinoxalino[2,3-*b*]chlorin 11. 2,3,12,13-Tetraoxo-5,10,15,20-tetrakis(3,5-di-*tert*-butylphenyl)bacteriochlorin **9** (234 mg, 0.208 mmol) was dissolved in dichloromethane (160 cm^3) and the solution stirred. 1,2-Diamino-4-nitrobenzene **4** (19 mg, 0.124 mmol) was dissolved in pyridine (5 cm^3) and gradually added to the stirring dichloromethane solution over 3 h. The solution was then allowed to stir for an additional 48 h. The solvent was evaporated to dryness and the crude residue was purified by chromatography over silica (dichloromethane–light petroleum; 1 : 2). The first major band was collected and the solvent removed to yield *anti*- and *syn*-linear bisnitroquinoxalino-porphyrins **10** (30 mg, 11%) as a brown microcrystalline solid, mp >300 °C. An analytically pure sample was obtained by recrystallisation from a dichloromethane–methanol solution (found: C, 74.2; H, 6.9; N, 9.9. $C_{88}H_{96}N_{10}O_4 + CH_2Cl_2$ requires C, 74.3; H, 6.8; N, 9.6%); $\nu_{max}(CHCl_3)/cm^{-1}$ 3389w, 2964s, 1723m, 1594m, 1531m, 1470m, 1346s, 1296m, 1261m and 1070m; $\lambda_{max}(CH_2Cl_2)/nm$ 362 (log ε 4.55), 423 (5.20), 462sh (5.00), 550 (4.25), 623 (4.15) and 674 (3.82); δ_H(400 MHz; $CDCl_3$) −2.45 (2 H, br s, inner NH), 1.52 (72 H, s, *t*-butyl H), 7.95 (1 H, br s, aryl H), 7.98 (1 H, br s, aryl H), 7.94–8.00 (10 H, m, aryl and H-8′ and H-8″ or H-5″), 8.03–8.04 (2 H, m, aryl H), 8.55 (2 H, dd, *J* 9.2 and 2.4, H-7′ and H-7″ or H-6″), 8.74 (2 H, d, *J* 2.4, H-5′ and H-5″ or H-7″) and 9.15–9.17 (4 H, m, β-pyrrolic H); *m*/*z* (MALDI-TOF) 1358.0 (M^+ requires 1357.8).

The second major band was collected and the solvent removed to yield 12,13-dioxo-5,10,15,20-tetrakis(3,5-di-*tert*-butylphenyl)-6′-nitroquinoxalino[2,3-*b*]chlorin **11** (109 mg, 42%) as a brownish–green microcrystalline solid, mp >300 °C (FAB-HRMS found: M^+ 1239.7289. $C_{82}H_{93}N_7O_4$ requires 1239.7314); $\nu_{max}(CHCl_3)/cm^{-1}$ 3393w, 2964s, 2869m, 2360w, 1733s, 1594m, 1533s, 1466m, 1364m, 1347s, 1296m, 1248m and 1070m; $\lambda_{max}(CH_2Cl_2)/nm$ 370sh (log ε 4.63), 409 (5.14), 627 (3.79), 681 (3.82) and 721 (3.74); δ_H(400 MHz; $CDCl_3$) −2.05 (2 H, br s, inner NH), 1.46 (16 H, s, *t*-butyl H), 1.47–1.48 (56 H, m, *t*-butyl H), 7.74 (4 H, d, *J* 1.6, aryl H), 7.77 (2 H, t, *J* 1.6, aryl H), 7.89–7.91 (5 H, m, aryl H and H-8′), 7.94 (1 H, t, *J* 1.6, aryl H), 7.99 (1 H, t, *J* 1.6, aryl H), 8.51 (1 H, dd, $J_{7',8'}$ 9.2, $J_{7',5'}$ 2.4, H-7′), 8.67–8.68 (2 H, m, β-pyrrolic H), 8.70 (1 H, d, $J_{5',7'}$ 2.4, H-5′) and 8.91–8.94 (2 H, m, β-pyrrolic H); *m*/*z* (MALDI-TOF) 1242.0 (M^+ requires 1240.7).

The third major band was collected and the solvent removed to give unreacted 2,3,12,13-tetraoxo-5,10,15,20-tetrakis(3,5-di-*tert*-butylphenyl)bacteriochlorin **9** (110 mg), mp >300 °C, which co-chromatographed with and had an identical ^{1}H NMR spectrum to an authentic sample.[32]

7‴″- and 6‴″-Nitroquinoxalino-appended bis-6″,6‴-biquinoxalinyl bis-porphyrins 12. 12,13-Dioxo-5,10,15,20-tetrakis(3,5-di-*tert*-butylphenyl)-6′-nitroquinoxalino[2,3-*b*]chlorin **11** (474 mg, 0.382 mmol) and 5,10,15,20-tetrakis(3,5-di-*tert*-butylphenyl)-6′-(3″,4″-diaminophenyl)quinoxalino[2,3-*b*]porphyrin **7** (487 mg, 0.383 mmol) were dissolved in chloroform (35 cm^3) and stirred for 3 days. The solvent was evaporated to dryness and the crude product purified by chromatography over silica (chloroform–light petroleum; 1 : 2). The major band was collected and the solvent removed to give 7‴″- and 6‴″-nitroquinoxalino-appended bis-6″,6‴-biquinoxalinyl bis-porphyrins **12** (137 mg, 94%) as green crystals, mp >300 °C. An analytically pure sample was obtained by recrystallisation from a chloroform–methanol solution (found: C, 79.95; H, 7.7; N, 8.2. $C_{170}H_{191}N_{15}O_2 + 0.75$ $CHCl_3$ requires C, 80.3; H, 7.5; N, 8.2%); $\nu_{max}(CHCl_3)/cm^{-1}$ 3383w, 2964s, 2858m, 2360m, 1733m, 1594m, 1476m, 1363m and 1296m; $\lambda_{max}(CH_2Cl_2)/nm$ 412sh (log ε 5.31), 443 (5.49), 472sh (5.33), 538 (4.67), 602 (4.26), 621 (4.32) and 673 (3.96); δ_H(400 MHz; $CDCl_3$) −2.44 (2 H, br s, inner NH), −2.42 (2 H, br s, inner NH), 1.50–1.55 (112 H, m, *t*-butyl H), 1.58–1.60 (32 H, m, *t*-butyl H), 7.82 (2 H, d, *J* 1.2, biquinoxalinyl H), 7.95–8.07 (22 H, m, 18 × aryl H and 4 × biquinoxalinyl H), 8.10–8.14 (5 H, m, 4 × aryl H and H-8‴″ *syn*-regioisomer or H-5‴″ *anti*-regioisomer), 8.16–8.19 (2 H, m, aryl H), 8.53 (1 H, dd, *J* 9.1 and 2.0, H-7‴″ *syn*-regioisomer or H-6‴″ *anti*-regioisomer), 8.77 (1 H, d, *J* 2.0, H-5‴″ *syn*-regioisomer or H-8‴″ *anti*-regioisomer), 8.80 (2 H, s, H-8′ and H-17′), 9.00–9.02 (2 H, m, H-7′ and H-18′), 9.09–9.10 (2 H, m, H-7 and H-18) and 9.14 (4 H, br s, H-8 and H-17); *m*/*z* (MALDI-TOF) 2476.4 (M^+ requires 2476.4).

Hexafluorophosphate[monogold(III) 7‴″- and 6‴″-nitroquinoxalino-appended bis-6″,6‴-biquinoxalinyl bis-porphyrins] 13. 7‴″- and 6‴″-Nitroquinoxalino-appended bis-6″,6‴-biquinoxalinyl bis-porphyrins **12** (250 mg, 0.101 mmol), potassium tetrachloroaurate(III) (100 mg, 0.264 mmol) and sodium acetate (80 mg, 1.48 mmol) were dissolved in a solution of chloroform (10 cm^3) and glacial acetic acid (18 M, 10 cm^3) and the reaction mixture heated at reflux for 24 h under nitrogen. The solution was then allowed to cool and fresh potassium tetrachloroaurate(III) (100 mg, 0.264 mmol) and sodium acetate (80 mg, 1.48 mmol) was added with additional glacial acetic acid (18 M, 1 cm^3). The mixture was then heated at reflux for another 24 h under nitrogen, allowed to cool and further potassium tetrachloroaurate(III) (110 mg, 0.290 mmol), sodium acetate (82 mg, 1.52 mmol) and glacial acetic acid (18 M, 1 cm^3) were added. The mixture was then heated at reflux for a further 24 h under nitrogen, allowed to cool and then the mixture was diluted with chloroform (150 cm^3). The mixture was washed with water (2 × 100 cm^3), sodium carbonate solution (10%, 2 × 100 cm^3), water (2 × 100 cm^3), dried over anhydrous sodium sulfate and filtered. The filtrate was evaporated to dryness and the residue dissolved in chloroform (10 cm^3). The organic phase was then stirred with a saturated solution of potassium hexafluorophosphate (2.02 g, 10.9 mmol) in water (10 cm^3) for 18 h. The mixture was then diluted with chloroform (100 cm^3) and washed with water (4 × 100 cm^3), dried over anhydrous sodium sulfate and filtered. The filtrate was removed under a vacuum and the residue purified by chromatography over silica (chloroform then increased to chloroform–methanol; 100 : 7). The first major band was collected and the solvent removed to give unreacted 7‴″- and 6‴″-nitroquinoxalino-appended bis-6″,6‴-biquinoxalinyl bis-porphyrins **12** (151 mg).

The second major band was collected and the solvent removed to yield hexafluorophosphate[monogold(III) 7‴″- and 6‴″-nitroquinoxalino-appended bis-6″,6‴-biquinoxalinyl bis-porphyrins] **13** (56 mg, 20%) as a reddish–brown solid, mp >300 °C (FAB-HRMS found: $[M - PF_6]^+$ 2671.4. $C_{170}H_{189}N_{15}O_2Au$ requires 2671.4676); $\nu_{max}(CHCl_3)/cm^{-1}$ 3382w, 2964s, 2928s, 2865m, 1731m, 1594s, 1533w, 1476m, 1465m, 1429w, 1394w, 1364m, 1347m, 1298m, 1247m and 1228w; $\lambda_{max}(CHCl_3)/nm$ 409brsh (log ε 5.12), 429sh (5.26), 447 (5.42), 548 (4.61), 588 (4.31), 614sh (4.20), 621 (4.28) and 673 (3.92);

δ_H(400 MHz; $CDCl_3$) −2.42 (1 H, s, inner NH), −2.41 (1 H, s, inner NH), 1.50–1.55 (108 H, m, *t*-butyl H), 1.57 (18 H, s, *t*-butyl H), 1.59 (18 H, s, *t*-butyl H), 7.91–7.92 (2 H, m, aryl H), 7.94–8.14 (26 H, m, 22 × aryl H, 3 × biquinoxalinyl and quinoxalino H), 8.21 (1 H, d, *J* 1.8, H-5‴ or H-5″), 8.25 (1 H, d, *J* 1.8, H-5‴ or H-5″), 8.31 (1 H, dd, $J_{7''',8'''}$ 8.8, $J_{7''',5'''}$ 1.8, H-7‴), 8.53 (1 H, dd, *J* 9.2 and 2.5, H-7‴″ *syn* regioisomer or H-6‴″ *anti* regioisomer), 8.77 (1 H, d, *J* 2.5, H-5‴″ *syn* regioisomer or H-8‴″ *anti* regioisomer), 9.13–9.15 (4 H, m, β-pyrrolic H on FbP), 9.24 (2 H, s, H-12′ and H-13′ on AuP), 9.25–9.26 (2 H, m, β-pyrrolic H on AuP), 9.33 (1 H, d, *J* 5.1, β-pyrrolic H on AuP) and 9.34 (1 H, d, *J* 5.2, β-pyrrolic H on AuP); δ_p(162 MHz; $CDCl_3$) −145.34 (1 P, h, *J* 713, PF_6); *m*/*z* (MALDI-TOF) 2671.2 ($[M - PF_6]^+$ requires 2671.4).

7‴″- and 6‴″-Aminoquinoxalino-appended bis-6″,6‴-biquinoxalinyl bis-porphyrins 14. 7‴″- and 6‴″-Nitroquinoxalino-appended bis-6″,6‴-biquinoxalinyl bis-porphyrins **12** (117 mg, 0.047 mmol) and tin(II) chloride dihydrate (100 mg, 0.4 mmol) were dissolved in chloroform (10 cm^3). Hydrochloric acid (10 M, 0.2 cm^3) was then added and the mixture stirred in the dark under nitrogen for 3 days. The mixture was then diluted with chloroform (100 cm^3) and washed with water (2 × 100 cm^3), sodium carbonate solution (10%, 2 × 100 cm^3) and water (2 × 100 cm^3), dried over anhydrous sodium sulfate and filtered. The filtrate was evaporated to dryness to yield crude 7‴″- and 6‴″-aminoquinoxalino-appended bis-6″,6‴-biquinoxalinyl bis-porphyrins **14** (110 mg, 95%) as a brownish–green solid, mp >300 °C. These compounds were used immediately in subsequent reactions due to extreme instability and were thus unable to be fully characterised. $\nu_{max}(CHCl_3)/cm^{-1}$ 3382s, 2963s, 1725s, 1631m, 1593s, 1550w, 1475m, 1427w, 1363m, 1296s, 1248m and 1118s; *m*/*z* (MALDI-TOF) 2447.5 (M^+ requires 2447.5).

Monogold(III) 7‴″- and 6‴″-aminoquinoxalino-appended bis-6″,6‴-biquinoxalinyl bis-porphyrins 15. Hexafluorophosphate[monogold(III) 7‴″- and 6‴″-nitroquinoxalino-appended bis-6″,6‴-biquinoxalinyl bis-porphyrins] **12** (102 mg, 0.038 mmol) and tin(II) chloride dihydrate (100 mg, 0.442 mmol) were dissolved in chloroform (15 cm^3). Hydrochloric acid (10 M, 0.25 cm^3) was then added and the reaction mixture stirred for 3 days under nitrogen. Chloroform (100 cm^3) was then added and the mixture washed with water (2 × 100 cm^3), sodium carbonate solution (10%, 2 × 100 cm^3) and water (2 × 100 cm^3), dried over anhydrous sodium sulfate, filtered and the solvent evaporated to dryness to give crude monogold(III) 7‴″- and 6‴″-aminoquinoxalino-appended bis-6″,6‴-biquinoxalinyl bis-porphyrins **15** (100 mg, 99%) as a reddish–brown solid, mp >300 °C; $\nu_{max}(CHCl_3)/cm^{-1}$ 3390m, 3385m, 2961s, 2863m, 1724m, 1624m, 1594m, 1467m, 1365m, 1296w, 1243m, 1117m and 1034w; δ_H(400 MHz; $CDCl_3$) −2.43 (1 H, s, inner NH), −2.41 (1 H, s, inner NH), 1.49–1.55 (108 H, m, *t*-butyl H), 1.57 (18 H, s, *t*-butyl H), 1.59 (18 H, s, *t*-butyl H), 5.08–5.38 (2 H, br m, NH_2), 6.90 (1 H, d, *J* 2.3, H-5‴″ *syn*-regioisomer or H-8‴″ *anti*-regioisomer), 7.20 (1 H, dd, *J* 8.8 and 2.5, H-7‴″*syn*-regioisomer or H-6‴″ *anti*-regioisomer), 7.62 (1 H, d, *J* 8.8, H-8‴″ *syn*-regioisomer or H-5‴″ *anti*-regioisomer), 7.90–7.93 (2 H, m, aryl H), 7.98–8.11 (25 H, m, 22 × aryl H and 3 × biquinoxalinyl H), 8.22 (1 H, d, *J* 1.8, H-5‴ or H-5″), 8.25 (1 H, d, *J* 1.8, H-5‴ or H-5″), 8.32 (1 H, dd, $J_{7''',8'''}$ 8.9, $J_{7''',5'''}$ 1.9, H-7‴), 9.09–9.10 (4 H, m, β-pyrrolic H on FbP), 9.21–9.25 (4 H, m, β-pyrrolic H on AuP), 9.32 (1 H, d, *J* 5.1, β-pyrrolic H on AuP) and 9.33 (1 H, d, *J* 5.1, β-pyrrolic H on AuP); *m*/*z* (MALDI-TOF) 2641.8 (M^+ requires 2641.4).

Zinc(II)–gold(III) tris-porphyrins 1. Monogold(III) 7‴″- and 6‴″-aminoquinoxalino-appended bis-6″,6‴-biquinoxalinyl bis-porphyrins **15** (142 mg, 0.054 mmol) and 5,10,15,20-tetrakis(3,5-di-*tert*-butylphenyl)-6′-aminoquinoxalino[2,3-*b*]porphyrin **5** (128 mg, 0.108 mmol) were dissolved in tetrahydrofuran (10 cm^3) and nitrogen was bubbled through the solution for 10 min. Hydrochloric acid (10 M, 1.8 cm^3) in ethanol (3 cm^3) was then added and nitrogen was passed over the solution for 10 min. Formaldehyde solution (37%, 0.45 cm^3) was added and the reaction mixture was stirred under nitrogen for 3.5 days and heated at 70–80 °C. The mixture was then diluted with chloroform (100 cm^3) and washed with water (2 × 100 cm^3), sodium carbonate solution (10%, 2 × 100 cm^3) and water (2 × 100 cm^3), dried over anhydrous sodium sulfate, filtered and the solvent evaporated to dryness. Analysis of the crude reaction mixture indicated the presence of bis-, tris- and tetrakis-porphyrin arrays. *m*/*z* (MALDI-TOF) 5319 (digold(III) tetrakis-porphyrin: M^+ requires 5318.8), 3858 (monogold(III) tris-porphyrin: M^+ requires 3858.1) and 2395 (free-base bis-porphyrin: M^+ requires 2397.4).

The mixture of bis-, tris- and tetrakis-porphyrin arrays (260 mg) were dissolved in chloroform (17 cm^3) and methanol (3 cm^3) and the mixture heated to reflux. Zinc(II) acetate dihydrate (105 mg, 0.476 mmol) was then added gradually over 3 h to the refluxing mixture. Once the addition of zinc(II) acetate dihydrate was complete the mixture was then heated at reflux for a further 1 h. Chloroform (100 cm^3) was then added and the mixture washed with water (4 × 100 cm^3), dried over anhydrous sodium sulfate and filtered. The filtrate was evaporated to dryness and the residue dissolved in chloroform (10 cm^3). The organic phase was then stirred with a saturated solution of potassium hexafluorophosphate (2.20 g, 11.9 mmol) in water (10 cm^3) for 18 h. Chloroform was then added (100 cm^3) and the mixture washed with water (4 × 100 cm^3), dried over anhydrous sodium sulfate and filtered. The filtrate was removed under a vacuum and the residue purified by chromatography over silica (chloroform–methanol; 100 : 1 then increased to chloroform–methanol; 100 : 8). The first band was collected and the solvent removed under a vacuum to give dizinc(II) extended Tröger's base bis-porphyrin **16** (90 mg, 66%) as a brown microcrystalline solid, mp >300 °C, which co-chromatographed and had an identical ^{1}H NMR spectrum to an authentic sample.[26]

The second band obtained from chromatography over silica was collected and the solvent removed under vacuum. The residue was purified by size exclusion chromatography (biobeads SX-1; toluene) and the first major band was collected and the solvent evaporated to dryness to afford zinc(II)–gold(III) tris-porphyrins **1** (118 mg, 54%) as a reddish–brown microcrystalline solid, mp >300 °C. An analytically pure sample was obtained by reverse phase HPLC on a Altech Altima C18 column (flow rate 7.0 cm^3 min^{-1}; chloroform–methanol; 30 : 100 then increased to chloroform–methanol; 80 : 20 over 1 h); $\nu_{max}(CHCl_3)/cm^{-1}$ 3692w, 3605w, 3383w, 2964s, 2868m, 1736w, 1681w, 1594s, 1547w, 1477m, 1427w, 1394w, 1364m, 1297w, 1247w, 1225s, 1214w, 1196w and 1168w; $\lambda_{max}(CHCl_3)$/nm 407 (log ε 5.36), 421 (5.40), 464 (5.65), 540 (4.77), 567 (4.68), 613 (4.58) and 670 (4.01); δ_H(400 MHz; $CDCl_3$) −2.45 (1 H, s, inner NH), −2.43 (1 H, s, inner NH), 1.33–1.34 (12 H, m, *t*-butyl H), 1.49–1.60 (180 H, m, *t*-butyl H), 1.63–1.66 (24 H, m, *t*-butyl H), 4.45 (2 H, br s, bridging H), 4.55 (1 H, d, J_{gem} 18.2, bridging H), 4.56 (1 H, d, J_{gem} 18.2, bridging H), 4.79 (1 H, d, J_{gem} 18.2, bridging H), 4.83 (1 H, d, J_{gem} 18.2, bridging H), 7.60–7.69 (5 H, m, 4 × quinoxalino H and 1 × aryl H), 7.77 (1 H, t, *J* 1.7, aryl H), 7.80 (1 H, t, *J* 1.7, aryl H), 7.85–7.86 (1 H, m, aryl H), 7.87–7.94 (7 H, m, aryl H), 7.96–8.03 (9 H, m, aryl H and biquinoxalinyl H), 8.04–8.06 (5 H, m, aryl H and biquinoxalinyl H), 8.07–8.13 (12 H, m, aryl H and biquinoxalinyl H), 8.15–8.17 (2 H, m, aryl H or biquinoxalinyl H), 8.21 (1 H, t, *J* 1.9, biquinoxalinyl H), 8.25 (1 H, d, *J* 1.7, biquinoxalinyl H), 8.32–8.33 (1 H, m, biquinoxalinyl H), 8.79 (1 H, d, *J* 4.7, β-pyrrolic H), 8.88–8.90 (3 H, m, β-pyrrolic H), 8.96 and 9.00 (2 H, ABq, J_{AB} 4.7, β-pyrrolic H), 8.99 (1 H, d, *J* 4.6, β-pyrrolic H), 9.08 (2 H, dd, *J* 4.6 and 1.7, β-pyrrolic H), 9.09–9.12 (1 H, m, β-pyrrolic H), 9.24 (2 H, s, β-pyrrolic H on AuP), 9.25–9.27 (2 H, m, β-pyrrolic H on AuP), 9.34 (1 H, d, *J* 5.0, β-pyrrolic H on AuP) and 9.35 (1 H, d, *J* 4.8, β-pyrrolic H on AuP); δ_p(162 MHz; $CDCl_3$) −145.34 (1 P, h, *J* 713, PF_6); *m*/*z* (MALDI-TOF) 3921.5 ($[M - PF_6]^+$ requires 3921.5).

The second band obtained from size exclusion chromatography, which eluted after the tris-porphyrin arrays, was collected and the solvent removed under a vacuum. MALDI-TOF mass spectrometry analysis indicated the presence of a variety of decomposed bis-porphyrins derived from **15**. *m/z* (MALDI-TOF) 2696, 2667 and 2804.

The third band obtained from chromatography over silica was collected and the solvent removed under vacuum to give impure digold(III) tetrakis-porphyrins **19** (45 mg, 30%). This compound was unable to be characterised as it rapidly decomposed. *m/z* (MALDI-TOF) 5417, 5319, 2820, 2681 and 1547 (M^+ requires 5318.8).

Zinc(II)–gold(III) tetrakis-porphyrins 2. Monogold(III) 7‴″- and 6‴″-aminoquinoxalino-appended bis-6″,6‴-biquinoxalinyl bis-porphyrins **15** (180 mg, 0.037 mmol) and 7‴″- and 6‴″-aminoquinoxalino-appended bis-6″,6‴-biquinoxalinyl bis-porphyrins **14** (180 mg, 0.074 mmol) were dissolved in tetrahydrofuran (12 cm^3) and nitrogen was bubbled through the solution for 10 min. Hydrochloric acid (10 M, 1.8 cm^3) in ethanol (3 cm^3) was then added and nitrogen was passed over the solution for 10 min. Formaldehyde solution (37%, 0.45 cm^3) was added and the reaction mixture was stirred under nitrogen for 5.5 days and heated at 70–80 °C. The mixture was then diluted with chloroform (100 cm^3) and washed with water (2 × 100 cm^3), sodium carbonate solution (10%, 2 × 100 cm^3) and water (2 × 100 cm^3), dried over anhydrous sodium sulfate, filtered and the solvent evaporated to dryness. Analysis of the crude reaction mixture indicated the presence of digold(III), monogold(III) and free base tetrakis-porphyrin arrays. *m/z* (MALDI-TOF) 5319 (digold(III) tetrakis-porphyrin: M^+ requires 5318.8), 5125 (monogold(III) tetrakis-porphyrin: M^+ requires 5123.9) and 4929 (free-base tetrakis-porphyrin: M^+ requires 4928.9).

The mixture of digold(III), monogold(III) and free base tetrakis-porphyrin arrays (270 mg) were dissolved in a solution of chloroform (15 cm^3) and methanol (2 cm^3). Zinc(II) acetate dihydrate (100 mg, 0.456 mmol) was then added and the mixture stirred at room temperature for 6 h. The mixture was then diluted with chloroform (100 cm^3) and washed with water (4 × 100 cm^3), dried over anhydrous sodium sulfate and filtered. The filtrate was evaporated to dryness and the residue dissolved in chloroform (10 cm^3). The organic phase was then stirred with a saturated solution of potassium hexafluorophosphate (2.14 g, 11.6 mmol) in water (10 cm^3) for 22 h. Chloroform (100 cm^3) was then added and the mixture washed with water (4 × 100 cm^3), dried over anhydrous sodium sulfate, filtered and the solvent removed under a vacuum. The residue was then purified by chromatography over silica (chloroform–methanol; 100 : 2 then increased to chloroform–methanol; 100 : 6). The first band was collected, the solvent removed and the residue repurified by size exclusion chromatography (biobeads SX-1; toluene).

The front running band was then collected and the solvent removed to afford dizinc(II) tetrakis-porphyrins **18** (65 mg, 35%) as reddish–brown crystals, mp >300 °C; $\nu_{max}(CHCl_3)/cm^{-1}$ 3691w, 3604w, 3328w, 2964s, 2927s, 2856m, 1721w, 1594s, 1549w, 1476m, 1466m, 1427w, 1393w, 1363m, 1346w, 1297m, 1248m, 1229w, 1194w, 1146w, 1118m, 1066w and 1038w; $\lambda_{max}(CHCl_3)/nm$ 424 (log ε 5.50), 467 (5.68), 538 (4.91), 572 (4.72), 616 (4.78) and 669 (4.21); δ_H(400 MHz; $CDCl_3$) −2.44 (4 H, br s, inner NH), 1.36 (9 H, br s, *t*-butyl H), 1.50–1.61 (252 H, m, *t*-butyl H), 1.65–1.69 (27 H, m, *t*-butyl H), 4.45 (2 H, br s, bridging H), 4.54 (2 H, d, J_{gem} 17.5, bridging H), 4.80 (2 H, d, J_{gem} 17.5, bridging H), 7.61–7.67 (4 H, m, quinoxalino H), 7.80–7.82 (4 H, m, aryl H), 7.92–7.93 (5 H, m, aryl H), 7.97–8.06 (28 H, m, aryl H and biquinoxalinyl H), 8.08–8.09 (3 H, m, aryl H), 8.10–8.12 (9 H, m, aryl H and possible biquinoxalinyl H), 8.14–8.16 (7 H, m, aryl H and biquinoxalinyl H), 8.19–8.20 (2 H, m, biquinoxalinyl H), 8.24 (2 H, d, *J* 1.6, biquinoxalinyl H), 8.88–8.91 (2 H, m, β-pyrrolic H), 8.92 (4 H, s, β-pyrrolic H), 9.01–9.03 (5 H, m, β-pyrrolic H), 9.07–9.09 (7 H, m, β-pyrrolic H) and 9.11–9.13 (2 H, m, β-pyrrolic H); *m/z* (MALDI-TOF) 5056.1 (M^+ requires 5055.7).

The second band obtained from chromatography over silica was collected and the solvent removed under a vacuum. The residue was then purified by size exclusion chromatography (biobeads SX-1; toluene) and the first major band collected to give zinc(II)–gold(III) tetrakis-porphyrins **2** (83 mg, 42%) as a reddish–brown microcrystalline solid, mp >300 °C. An analytically pure sample was obtained by reverse phase HPLC on an Altech Altima C18 column (flow rate 7.0 cm^3 min^{-1}; chloroform–methanol; 30 : 100 then increased to chloroform–methanol; 80 : 20 over 45 min); $\nu_{max}(CHCl_3)/cm^{-1}$ 3695w, 3608w, 3381w, 2963s, 2950s, 2861m, 1719s, 1594m, 1549w, 1490w, 1476m, 1463m, 1427w, 1392w, 1381w, 1364m, 1343w, 1293s, 1248m, 1222w, 1201w, 1194w, 1145m, 1120m, 1074m and 1040w; $\lambda_{max}(CHCl_3)/nm$ 413sh (log ε 5.45), 431sh (5.49), 446sh (5.59), 467 (5.73), 539 (4.94), 571 (4.66), 616 (4.73) and 670 (4.26); δ_H(400 MHz; $CDCl_3$) −2.44 (4 H, br s, inner NH), 1.30–1.39 (27 H, m, *t*-butyl H), 1.50–1.60 (243 H, m, *t*-butyl H), 1.64–1.72 (18 H, m, *t*-butyl H), 4.45 (2 H, br s, bridging H), 4.54 (2 H, d, J_{gem} 17.5, bridging H), 4.79 (2 H, d, J_{gem} 17.5, bridging H), 7.61–7.67 (4 H, m, quinoxalino H), 7.80–7.81 (2 H, m, aryl H), 7.92–7.93 (6 H, m, aryl H), 7.97–8.06 (25 H, m, aryl H and biquinoxalinyl H), 8.07–8.08 (3 H, m, aryl H), 8.10–8.11 (12 H, m, aryl H and biquinoxalinyl H), 8.12–8.16 (6 H, m, aryl H and biquinoxalinyl H), 8.18–8.19 (2 H, m, biquinoxalinyl H), 8.21–8.22 (1 H, m, biquinoxalinyl H), 8.23 (2 H, d, *J* 1.5, biquinoxalinyl H), 8.30–8.33 (1 H, m, biquinoxalinyl H), 8.87–8.90 (2 H, m, β-pyrrolic H), 8.91 (2 H, s, β-pyrrolic H), 9.01–9.03 (2 H, m, β-pyrrolic H), 9.05–9.08 (6 H, m, β-pyrrolic H), 9.10–9.12 (2 H, m, β-pyrrolic H), 9.22–9.24 (4 H, m, β-pyrrolic H) and 9.30–9.33 (2 H, m, β-pyrrolic H); δ_p(162 MHz; $CDCl_3$) −145.34 (1 P, h, *J* 713, PF_6); *m/z* (MALDI-TOF) 5187.3 ($[M - PF_6]^+$ requires 5187.3).

The third band obtained from chromatography over silica was collected and the solvent removed under a vacuum to give impure digold(III) tetrakis-porphyrins **17** (18 mg, 17%) as a reddish–brown microcrystalline solid. This compound was unable to be characterised as it rapidly decomposed. *m/z* (MALDI-TOF) 5417, 5319, 2820, 2681 and 1547 (M^+ requires 5318.8).

During size exclusion chromatography the second band, which eluted after the tetrakis-porphyrin arrays, was collected and the solvent removed under vacuum. MALDI-TOF mass spectrometry analysis indicated the presence of a variety of bis-porphyrin impurities. *m/z* (MALDI-TOF) 2741, 2541 and 1489.

5,10,15,20-Tetrakis(3,5-di-*tert*-butylphenyl)-6′-nitroquinoxalino[2,3-*b*]quinoxalino[12,13-*b*′]porphyrin 20. 12,13-Dioxo-5,10,15,20-tetrakis(3,5-di-*tert*-butylphenyl)-6′-nitroquinoxalino-[2,3-*b*]chlorin **11** (101 mg, 0.0818 mmol) and *o*-phenylenediamine **19** (55 mg, 0.510 mmol) were dissolved in chloroform (12 cm^3) and the mixture stirred for 24 h. The solvent was removed under vacuum and the residue purified by chromatography over silica (chloroform–light petroleum; 1 : 2). The major front running band was collected and evaporated to dryness. The residue was recrystallised from a dichloromethane-methanol solution to afford 5,10,15,20-tetrakis(3,5-di-*tert*-butylphenyl)-6′-nitroquinoxalino[2,3-*b*]quinoxalino[12,13-*b*′]porphyrin **20** (80 mg, 75%) as a red microcrystalline solid, mp >300 °C (found: C, 80.2; H, 7.4; N, 9.7. $C_{88}H_{97}N_9O_2$ requires C, 80.5; H, 7.45; N, 9.6%); $\nu_{max}(CHCl_3)/cm^{-1}$ 3689w, 3598w, 3384w, 2964s, 2903m, 2867m, 1621w, 1594s, 1559w, 1533w, 1476m, 1428w, 1393w, 1362m, 1346s, 1296m, 1247m, 1201w, 1147m, 1110m and 1071m; $\lambda_{max}(CH_2Cl_2)/nm$ 353 (log ε 4.56), 408sh (4.95), 443 (5.22), 543 (4.29), 620 (4.14) and 672 (3.98); δ_H(400 MHz; $CDCl_3$) −2.45 (1 H, s, inner NH), −2.44 (1 H, s, inner NH), 1.50 (45 H, s, *t*-butyl H), 1.51 (18 H, s, *t*-butyl H), 1.55 (9 H, s, *t*-butyl H), 7.74–7.78 (2 H, m, quinoxalino H), 7.82–7.85 (2 H, m, quinoxalino H), 7.93–7.96 (4 H, m, aryl H and H-8′), 7.99–8.00 (7 H, m, aryl H), 8.02 (2 H, t, *J* 1.7,

aryl H), 8.52 (1 H, dd, $J_{7',8'}$ 9.2, $J_{7',5'}$ 2.5, H-7′), 8.76 (1 H, d, $J_{5',7'}$ 2.5, H-5′) and 9.11–9.13 (4 H, m, β-pyrrolic H); *m/z* (MALDI-TOF) 1312.7 (M^+ requires 1312.8).

5,10,15,20-Tetrakis(3,5-di-*tert*-butylphenyl)-6′-aminoquinoxalino[2,3-*b*]quinoxalino[12,13-*b*′]porphyrin 21. 5,10,15,20-Tetrakis(3,5-di-*tert*-butylphenyl)-6′-nitroquinoxalino[2,3-*b*]quinoxalino[12,13-*b*′]porphyrin **20** (80 mg, 0.061 mmol) and tin(II) chloride dihydrate (74 mg, 0.433 mmol) were dissolved in chloroform (10 cm^3). Hydrochloric acid (10 M, 0.4 cm^3) was then added and the mixture stirred under nitrogen in the dark for 3 days. The mixture was then diluted with chloroform (100 cm^3) and washed with water (2 × 100 cm^3), sodium carbonate solution (2 × 100 cm^3) and water (2 × 100 cm^3), dried over anhydrous sodium sulfate and filtered. The filtrate was evaporated to dryness to yield crude 5,10,15,20-tetrakis(3,5-di-*tert*-butylphenyl)-6′-aminoquinoxalino[2,3-*b*]quinoxalino[12,13-*b*′]porphyrin **21** (77 mg, 98%) as a reddish–brown powder, mp >300 °C. The compound was used immediately in the subsequent reaction due to instability and was thus unable to be fully characterised; $\nu_{max}(CHCl_3)/cm^{-1}$ 3501w, 3404m, 3382m, 2964s, 2903m, 2866m, 1631s, 1594s, 1549w, 1504m, 1476m, 1428w, 1363m, 1348w, 1346s, 1299m, 1247m, 1208w, 1169w and 1148w; δ_H(400 MHz; $CDCl_3$) −2.43 (1 H, s, inner NH), −2.40 (1 H, s, inner NH), 1.55 (72 H, br s, *t*-butyl H), 4.19 (2 H, s, NH_2), 6.94 (1 H, br s, H-5′), 7.24 (1 H, dd, $J_{7',8'}$ 8.8, $J_{7',5'}$ 2.0, H-7′), 7.66 (1 H, d, $J_{8',7'}$ 8.8, H-8′), 7.78–7.80 (2 H, m, quinoxalino H), 7.89–7.91 (2 H, m, quinoxalino H), 7.97 (2 H, br s, aryl H), 8.00 (2 H, br s, aryl H), 8.01–8.06 (8 H, m, aryl H) and 9.11–9.15 (4 H, m, β-pyrrolic H); *m/z* (MALDI-TOF) 1282.7 (M^+ requires 1282.8).

{5,5′,10,10′,15,15′,20,20′-Octakis(3,5-di-*tert*-butylphenyl)-4‴′*H*,8‴′*H*-1‴′,5‴′-methano[1‴′,5‴′]diazocino[2‴′,3‴′-*b*:6‴′,7‴′-*b*′]-quinoxalino[2,3-*b*]bisquinoxalino[2′,3′-*b*′:12′,13′-*b*′]bisporphyrinato}zinc(II) 23. 5,10,15,20-Tetrakis(3,5-di-*tert*-butylphenyl)-6′-aminoquinoxalino[2,3-*b*]porphyrin **5** (78 mg, 0.066 mmol) and 5,10,15,20-tetrakis(3,5-di-*tert*-butylphenyl)-6′-aminoquinoxalino[2,3-*b*]quinoxalino[12,13-*b*′]porphyrin **21** (80 mg, 0.0624 mmol) were dissolved in tetrahydrofuran (12 cm^3) and nitrogen was bubbled through the solution for 10 min. Hydrochloric acid (10 M, 1.8 cm^3) in ethanol (3.0 cm^3) was then added and nitrogen passed over the solution for 10 min. Formaldehyde solution (0.3 cm^3, 37%) was added and the mixture stirred under nitrogen and heated at 70–75 °C for 3 days. The mixture was then diluted with dichloromethane (100 cm^3) and washed with water (2 × 100 cm^3), sodium carbonate solution (2 × 100 cm^3) and water (2 × 100 cm^3), dried over anhydrous sodium sulfate and filtered. The filtrate was evaporated to dryness and the residue was purified by chromatography over silica (dichloromethane–light petroleum; 1 : 1). The major dark band was collected and the solvent removed to give a mixture of mono- and bis-appended quinoxaline extended Tröger's base bis-porphyrins and extended Tröger's base bis-porphyrin. *m/z* (MALDI-TOF) 2601 (bis-appended: M^+ requires 2601.6), 2499 (mono-appended: M^+ requires 2499.6) and 2398 (extended Tröger's base bis-porphyrin: M^+ requires 2397.4).

Zinc(II) acetate dihydrate (40 mg, 0.182 mmol) and the mixture of bis-porphyrins were dissolved in a solution of dichloromethane (14 cm^3) and methanol (2 cm^3). The mixture was then stirred in the dark for 8 h. The solvent was then evaporated to dryness without heating and the residue purified by chromatography over silica (chloroform–light petroleum; 1 : 1). The first major band was collected, the solvent removed and the residue recrystallised from a dichloromethane-methanol solution to give {5,5′,10,10′,15,15′,20,20′-octakis(3,5-di-*tert*-butylphenyl)-4‴′*H*,8‴′*H*-1‴′,5‴′-methano[1‴′,5‴′]diazocino[2‴′3‴′-*b*:6‴′,7‴′-*b*′]quinoxalino[2,3-*b*]bisquinoxalino[2′,3′-*b*′:12′,13′-*b*′]-bisporphyrinato}zinc(II) **23** (25 mg, 16%) as red crystals, mp >300 °C; $\nu_{max}(CHCl_3)/cm^{-1}$ 3690w, 3607w, 3381w, 2964s, 2904m, 2867m, 1594s, 1547w, 1477m, 1394w, 1364m, 1297m, 1247m, 1227m, 1201m, 1169w and 1152m; $\lambda_{max}(CH_2Cl_2)$/nm 354 (log ε 4.71), 408 (5.30), 456 (5.60), 535 (4.60), 568 (4.46), 613 (4.48) and 668 (4.06); δ_H(400 MHz; $CDCl_3$) −2.52 (1 H, s, inner NH), −2.50 (1 H, s, inner NH), 1.45–1.54 (108 H, m, *t*-butyl H), 1.63–1.65 (36 H, m, *t*-butyl H), 4.45 (2 H, s, H-9‴′), 4.54 (1 H, d, J_{gem} 17.6, H-4‴′ or H-8‴′), 4.55 (1 H, d, J_{gem} 17.6, H-4‴′ or H-8‴′), 4.79 (1 H, d, J_{gem} 17.6, H-4‴′ of H-8‴′), 4.82 (1 H, d, J_{gem} 17.6, H-4‴′ or H-8‴′), 7.60–7.68 (4 H, m, quinoxalino H), 7.73–7.75 (2 H, m, aryl H), 7.77 (1 H, t, *J* 1.8, aryl H), 7.79 (1 H, t, *J* 1.8, aryl H), 7.81–7.85 (2 H, m, quinoxalino H), 7.86 (1 H, t, *J* 1.8, aryl H), 7.89 (2 H, t, *J* 1.8, aryl H), 7.91 (1 H, t, *J* 1.8, aryl H), 7.92 (1 H, t, *J* 1.8, aryl H), 7.93–8.03 (9 H, m, aryl H and quinoxalino H), 8.05–8.07 (2 H, m, aryl H), 8.08–8.13 (3 H, m, aryl H), 8.14–8.17 (3 H, m, aryl H), 8.79 (1 H, d, *J* 4.7, β-pyrrolic H), 8.87 (1 H, dd, *J* 4.9 and 1.8, β-pyrrolic H), 8.90 (2 H, s, β-pyrrolic H), 8.97 and 9.00 (2 H, ABq, J_{AB} 4.7, β-pyrrolic H), 8.99 (1 H, d, *J* 4.7, β-pyrrolic H), 9.05 (2 H, d, *J* 1.8, β-pyrrolic H) and 9.09 (1 H, dd, *J* 4.9 and 1.8, β-pyrrolic H); *m/z* (MALDI-TOF) 2563.0 (M^+ requires 2562.9).

The second major band was collected, the solvent removed and the residue recrystallised from a dichloromethane–methanol solution to give dizinc(II) extended Tröger's base bis-porphyrin **16** (23 mg, 15%) as blue–purple crystals, mp >300 °C, which co-chromatographed and had an identical spectroscopic data to an authentic sample.[26]

Trace quantities of 5,10,15,20-tetrakis(3,5-di-*tert*-butylphenyl)-4‴′*H*,8‴′*H*-1‴′,5‴′-methano[1‴′,5‴′]diazocino[2‴′,3‴′-*b*:6‴′,7‴′-*b*]bisquinoxalino[2,3-*b*:12,13-*b*′]bisporphyrin **22** were detected by mass spectrometry in fractions collected before the elution of the first major band during column chromatography. *m/z* (MALDI-TOF) 2601.6 (M^+ requires 2601.6).

12,13-Dioxo-5,10,15,20-tetrakis(3,5-di-*tert*-butylphenyl)-[2,3-*b*]quinoxalinoporphyrin 24. 2,3,12,13-Tetraoxo-5,10,15,20-tetrakis(3,5-di-*tert*-butylphenyl)bacteriochlorin **9** (157 mg, 0.140 mmol) was dissolved in dichloromethane (150 cm^3) and stirred. *o*-Phenylenediamine **19** (7.6 mg, 0.0704 mmol) was dissolved in pyridine (5 cm^3) and gradually added over 5 h to the stirring dichloromethane solution. The solution was then stirred for a further 48 h. The solution was then removed under a vacuum and the residue purified by chromatography over silica (dichloromethane–light petroleum; 1 : 2). The first major band was collected and the solvent evaporated to dryness to give 5,10,15,20-tetrakis(3,5-di-*tert*-butylphenyl)bisquinoxalino[2,3-*b*:12,13-*b*]porphyrin **30** (20 mg, 11.5%) which co-chromatographed and had identical spectroscopic data to an authentic sample.[33]

The second major band was collected and the solvent evaporated to dryness to give 12,13-dioxo-5,10,15,20-tetrakis(3,5-di-*tert*-butylphenyl)[2,3-*b*]quinoxalino-porphyrin **24** (50 mg, 30%) which co-chromatographed and had identical spectroscopic data to an authentic sample.[33] $\nu_{max}(CHCl_3)/cm^{-1}$ 3690w, 3603w, 3392w, 2965s, 2904m, 2867m, 1732s, 1722s, 1594s, 1476m, 1428w, 1393w, 1363m, 1347s, 1297m, 1248m, 1219s, 1209s and 1084m; $\lambda_{max}(CHCl_3)$/nm 353.5 (log ε 4.53), 395sh (5.03), 419 (5.17), 483sh (4.35), 572.5sh (3.69), 622.5 (3.74), 677 (3.80) and 727 (3.80); δ_H(400 MHz; $CDCl_3$) −2.06 (2 H, s, inner NH), 1.46 (36 H, s, *t*-butyl H), 1.48 (36 H, s, *t*-butyl H), 7.72–7.81 (10 H, m, 6 × aryl H and 4 × quinoxalino H), 7.89 (4 H, d, *J* 1.8, aryl H), 7.91 (2 H, t, *J* 1.8, aryl H) 8.65 and 8.91 (4 H, ABq, J_{AB} 5.0, *J* 1.8, β-pyrrolic H).

The final band was collected and the solvent removed to give unreacted 2,3,12,13-tetraoxo-5,10,15,20-tetrakis(3,5-di-*tert*-butylphenyl)bacteriochlorin **9** (78 mg) which co-chromatographed and had identical spectroscopic data to an authentic sample prepared by Govenlock *et al*.[32]

Bis-6,6′-biquinoxalinyl[2,3-*b*]quinoxalino bis-porphyrin 25. 5,10,15,20-Tetrakis(3,5-di-*tert*-butylphenyl)-6′-(3″,4″-diaminophenyl)quinoxalino[2,3-*b*]porphyrin **7** (115 mg, 0.0905 mmol)

and 12,13-dioxo-5,10,15,20-tetrakis(3,5-di-*tert*-butylphenyl)-[2,3-*b*]quinoxalino-porphyrin **24** (107 mg, 0.0894 mmol) were dissolved in chloroform (10 cm^3) and the mixture stirred for 48 h. The solvent was evaporated to dryness and the crude product purified by chromatography over silica (chloroform–light petroleum; 1 : 1). The major band was collected, solvent removed and the residue recrystallised from a chloroform–methanol solution to give bis-6,6′-biquinoxalinyl-[2,3-*b*]-quinoxalino bis-porphyrin **25** (205 mg, 94%) as green crystals, mp >300 °C (found: C, 83.92; H, 8.01; N, 8.32. $C_{170}H_{192}N_{14}$ requires C, 83.98; H, 7.96; N, 8.06%); $\nu_{max}(CHCl_3)/cm^{-1}$ 3693w, 3601w, 3382w, 3339w, 2964s, 2904m, 2867m, 1593s, 1553w, 1476m, 1427w, 1393w, 1363m and 1297m; $\lambda_{max}(CHCl_3)$/nm 362sh (log ε 4.81), 409sh (5.31), 447sh (5.57), 457 (5.63), 535 (4.79), 570sh (4.09), 609sh (4.35), 614 (4.38) and 669 (4.14); δ_H(400 MHz; $CDCl_3$) −2.44 (2 H, br s, inner NH), −2.44 (2 H, br s, inner NH), 1.50 (18 H, s, *t*-butyl H), 1.51 (18 H, s, *t*-butyl H), 1.52 (18 H, s, *t*-butyl H), 1.53 (18 H, s, *t*-butyl H), 1.54 (18 H, s, *t*-butyl H), 1.55 (18 H, s, *t*-butyl H), 1.58–1.59 (36 H, m, *t*-butyl H), 7.74–7.78 (2 H, m, quinoxalino H), 7.81 (1 H, t, *J* 1.9, aryl H), 7.82 (1 H, t, *J* 1.9, aryl H), 7.83–7.86 (2 H, m, quinoxalino H), 7.95 (1 H, t, *J* 1.9, aryl H), 7.96 (1 H, t, *J* 1.9, aryl H), 7.97–8.02 (7 H, m, aryl H and biquinoxalinyl H), 8.03–8.06 (9 H, m, aryl H and biquinoxalinyl H), 8.07 (2 H, d, *J* 1.8, aryl H), 8.12–8.13 (5 H, m, aryl H × 4 and biquinoxalinyl H), 8.14–8.15 (1 H, m, biquinoxalinyl H), 8.17 (2 H, dd, *J* 1.8 and 5.0, biquinoxalinyl H), 8.81 (2 H, s, H-12 and H-13), 9.01–9.03 (2 H, s, β-pyrrolic H) and 9.10–9.13 (6 H, m, β-pyrrolic H); *m/z* (MALDI-TOF) 2435 (M^+ requires 2431).

Zinc(II){bis-6,6′-biquinoxalinyl[2,3-*b*]quinoxalino bis-porphyrin} 26. Bis-6,6′-biquinoxalinyl[2,3-*b*]quinoxalino bis-porphyrin **25** (100 mg, 0.0411 mmol) and zinc(II) acetate dihydrate (27 mg, 0.123 mmol) were dissolved in chloroform (11 cm^3) and methanol (1 cm^3). The mixture was then stirred in the dark for 8 h. The solvent was then removed under a vacuum and the residue purified by chromatography over silica (chloroform–light petroleum; 1 : 1). The major band was collected, the solvent removed and the residue recrystallised from a chloroform–methanol solution to afford zinc(II){bis-6,6′-biquinoxalinyl-[2,3-*b*]-quinoxalino bis-porphyrin} **26** (101 mg, 99%) as green crystals, mp >300 °C (found: C, 80.78; H, 7.27; N, 7.98. $C_{170}H_{190}N_{14}Zn + 2H_2O$ requires C, 80.68; H, 7.73; N, 7.75%); $\nu_{max}(CHCl_3)/cm^{-1}$ 3690w, 3605w, 3383w, 2964s, 2904m, 2867m, 1594s, 1553w, 1477m, 1458w, 1427w, 1393w, 1363m, 1346w and 1297m; $\lambda_{max}(CHCl_3)$/nm 358sh (log ε 4.77), 412sh (5.36), 423 (5.37), 458 (5.55), 536 (4.67), 572 (4.53), 615 (4.59) and 669 (4.13); δ_H(400 MHz; $CDCl_3$) −2.43 (2 H, br s, inner NH), 1.50–1.52 (54 H, m, *t*-butyl H), 1.53 (18 H, s, *t*-butyl H), 1.54 (18 H, s, *t*-butyl H), 1.545 (18 H, s, *t*-butyl H), 1.58 (18 H, s, *t*-butyl H), 1.59 (18 H, s, *t*-butyl H), 7.74–7.77 (2 H, m, quinoxalino H), 7.80–7.81 (2 H, m, aryl H), 7.83–7.86 (2 H, m, quinoxalino H), 7.95–7.96 (2 H, m, biquinoxalinyl H), 7.98–8.09 (18 H, m, aryl H, biquinoxalinyl H), 8.11 (4 H, t, *J* 1.9, aryl H), 8.14–8.24 (4 H, m, biquinoxalinyl H), 8.92 (2 H, s, β-pyrrolic H), 9.02 and 9.08 (2 H, ABq, J_{AB} 4.5, β-pyrrolic H), 9.03 and 9.09 (2 H, ABq, J_{AB} 4.5, β-pyrrolic H) and 9.12–9.13 (4 H, m, β-pyrrolic H); *m/z* (MALDI-TOF) 2498 (M^+ requires 2495).

Gold(III){bis-6,6′-biquinoxalinyl[2,3-*b*]quinoxalino bis-porphyrin} 27. Bis-6,6′-biquinoxalinyl-[2,3-*b*]-quinoxalino bis-porphyrin **25** (191 mg, 0.0787 mmol) was dissolved in chloroform (16 cm^3) and glacial acetic acid (15 cm^3). Potassium tetrachloroaurate(III) (93 mg, 0.246 mmol) and sodium acetate (71 mg, 0.866 mmol) were then added and the mixture heated at reflux for 24 h under nitrogen. The solution was then allowed to cool and fresh potassium tetrachloroaurate(III) (97 mg, 0.257 mmol) and sodium acetate (77 mg, 0.939 mmol) were added. The mixture was then heated at reflux for another 24 h under nitrogen, allowed to cool and further potassium tetrachloroaurate(III) (90 mg, 0.238 mmol) and sodium acetate (72 mg, 0.878 mmol) were added. The mixture was heated at reflux for a further 24 h under nitrogen, allowed to cool and the mixture was then diluted with chloroform (150 cm^3). The mixture was washed with water (2 × 200 cm^3), sodium carbonate solution (10%, 2 × 200 cm^3) and water (2 × 200 cm^3), dried over anhydrous sodium sulfate and filtered. The filtrate was removed under a vacuum and the residue dissolved in chloroform (15 cm^3). The organic phase was then stirred with a saturated solution of potassium hexafluorophosphate (2.32 g, 12.5 mmol) in water (10 cm^3) for 24 h. The mixture was then diluted with chloroform (100 cm^3) and washed with water (5 × 100 cm^3), dried over anhydrous sodium sulfate, filtered and the solvent evaporated to dryness. The residue was purified by chromatography over silica (chloroform then gradually increased to chloroform–methanol; 100 : 7). The front running band was collected and the solvent removed to give unreacted bis-6,6′-biquinoxalinyl-[2,3-*b*]-quinoxalino bis-porphyrin **25** (56 mg) which co-chromatographed to an authentic sample.

The major polar band was collected and the solvent removed to afford gold(III){bis-6,6′-biquinoxalinyl-[2,3-*b*]-quinoxalino bis-porphyrin} **27** (46.5 mg, 21%) as a reddish–green powder, mp >300 °C; $\nu_{max}(CHCl_3)/cm^{-1}$ 3692w, 3604w, 3383w, 2965s, 2905m, 2868m, 1722w, 1683w, 1594s, 1553w, 1477m, 1460w, 1429w, 1394w, 1364s, 1329w and 1298m; $\lambda_{max}(CHCl_3)$/nm 358 (log ε 4.76), 400 (4.99), 445brsh (5.34), 456 (5.36), 541 (4.57), 590 (4.29), 615 (4.27), 644brsh (3.89) and 669 (4.01); δ_H(400 MHz; $CDCl_3$) −2.43 (2 H, br s, inner NH), 1.50 (18 H, s, *t*-butyl H), 1.510 (18 H, s, *t*-butyl H), 1.514 (18 H, s, *t*-butyl H), 1.53 (18 H, s, *t*-butyl H), 1.54 (18 H, s, *t*-butyl H), 1.55 (18 H, s, *t*-butyl H), 1.58 (18 H, s, *t*-butyl H), 1.59 (18 H, s, *t*-butyl H), 7.75–7.78 (2 H, m, quinoxalino H), 7.83–7.87 (2 H, m, quinoxalino H), 7.91–7.92 (2 H, m, aryl H or biquinoxalinyl H), 7.95–7.97 (2 H, m, aryl H or biquinoxalinyl H), 7.99–8.03 (9 H, m, aryl H and biquinoxalinyl H), 8.04–8.12 (14 H, m, aryl H and biquinoxalinyl H), 8.22 (1 H, d, *J* 1.9, biquinoxalinyl H), 8.26 (1 H, d, *J* 1.9, biquinoxalinyl H), 8.33 (1 H, dd, *J* 2.0 and 8.9, biquinoxalinyl H), 9.12 and 9.13 (4 H, ABq, J_{AB} 4.5, β-pyrrolic H), 9.25 (2 H, br s, β-pyrrolic H), 9.26 and 9.35 (2 H, ABq, J_{AB} 5.2, β-pyrrolic H), 9.27 and 9.36 (2 H, ABq, J_{AB} 5.2, β-pyrrolic H); *m/z* (MALDI-TOF) 2631 ([M^+-PF_6] requires 2627).

Free-base tris- and tetrakis-porphyrins 31 and 32. Both 7‴- and 6‴-aminoquinoxalino-appended bis-6″,6‴-biquinoxalinyl bis-porphyrins **14** (300 mg, 0.123 mmol) and 5,10,15,20-tetrakis(3,5-di-*tert*-butylphenyl)-6′-aminoquinoxalino[2,3-*b*]-porphyrin **5** (146 mg, 0.123 mmol) were dissolved in tetrahydrofuran (18 cm^3) and nitrogen was bubbled through the solution for 10 min. Hydrochloric acid (10 M, 2.4 cm^3) in ethanol (3.6 cm^3) was then added and nitrogen was passed over the solution for 10 min. Formaldehyde solution (37%, 0.75 cm^3) was added and the reaction mixture was stirred under nitrogen for 2 days and heated at 60–70 °C. The solvent was then removed under a vacuum and the residue dissolved in chloroform (100 cm^3). The organic phase was then washed with water (2 × 100 cm^3), sodium carbonate solution (10%, 2 × 100 cm^3) and water (2 × 100 cm^3), dried over anhydrous sodium sulfate, filtered and the solvent evaporated to dryness. The residue was fractionated by chromatography over silica (chloroform–light petroleum; 1 : 1) and the major dark band was collected and the solvent removed to give a mixture of extended Tröger's base bis-porphyrin, tris-porphyrin arrays and tetrakis-porphyrin arrays. *m/z* (MALDI-TOF) 4928 (tetrakis-porphyrin: M^+ requires 4928.9), 3663 (tris-porphyrin: M^+ requires 3663.2) and 2395 (bis-porphyrin: M^+ requires 2397.4).

The mixture was then further purified by size exclusion chromatography (biobeads SX-1; toluene). The first band, that contained a mixture of tris- and tetrakis-porphyrin arrays, was carefully collected to enable separation of these multiporphyrin

arrays. The tetrakis-porphyrin arrays, which eluted first from the column, were collected and the solvent removed under a vacuum. The residue was then repurified by chromatography over silica (chloroform–light petroleum; 1 : 1). The major dark band was collected and the solvent removed to afford free-base tetrakis-porphyrins **32** (45 mg, 15%) as greenish–blue crystals, mp >300 °C. An analytically pure sample was obtained by recrystallisation from a chloroform–methanol solution (found: C, 82.1; H 8.1; N, 8.6. $C_{343}H_{386}N_{30}$ + $CHCl_3$ requires C, 81.8; H, 7.7; N, 8.3%); $\nu_{max}(CHCl_3)/cm^{-1}$ 3387w, 3349w, 3056w, 2964s, 2867m, 1699w, 1590s, 1550w, 1476m, 1427w, 1363m, 1298m, 1248w, 1221s and 1203m; $\lambda_{max}(CHCl_3)$/nm 410br sh (log ε 5.53), 444 (5.72), 467 (5.84), 536 (5.10), 567sh (4.42), 601sh (4.53), 615 (4.68) and 669 (4.33); δ_H(400 MHz; $CDCl_3$) −2.44 (8 H, br s, inner NH), 1.49–1.67 (288 H, m, *t*-butyl H), 4.45 (2 H, br s, bridging H), 4.54 (2 H, d, J_{gem} 17.8, bridging H), 4.80 (2 H, d, J_{gem} 17.8, bridging H), 7.61–7.68 (4 H, m, quinoxalino H), 7.81–7.82 (4 H, m, aryl H), 7.92–7.93 (3 H, m, aryl H), 7.94–8.08 (32 H, m, aryl H and biquinoxalinyl H), 8.10–8.20 (21 H, m, aryl H), 8.80 (4 H, s, β-pyrrolic H), 8.88–8.90 (2 H, m, β-pyrrolic H), 9.00–9.03 (4 H, m, β-pyrrolic H) and 9.06–9.14 (10 H, m, β-pyrrolic H); *m/z* (MALDI-TOF) 4928.3 (M^+ requires 4928.9).

The tris-porphyrin arrays that eluted after the tetrakis-porphyrin arrays in the first band during size exclusion chromatography were collected and the solvent removed under a vacuum. The residue was repurified by chromatography over silica (chloroform–light petroleum; 1 : 1) and the major band collected and the solvent removed to afford free-base tris-porphyrins **31** (92 mg, 21%) as greenish–blue crystals, mp >300 °C. An analytically pure sample was obtained by recrystallisation from a chloroform–methanol solution (found: C, 82.2; H, 8.1; N, 8.6. $C_{255}H_{290}N_{22}$ + 0.5 $CHCl_3$ requires C, 82.4; H, 7.9; N, 8.3%); $\nu_{max}(CHCl_3)/cm^{-1}$ 3339w, 3063w, 2964s, 2867m, 1699w, 1593s, 1550w, 1476m, 1393w, 1364m, 1296w and 1248s; $\lambda_{max}(CHCl_3)$/nm 414br sh (log ε 5.48), 440 (5.66), 462 (5.70), 535 (4.93), 567sh (4.28), 601 (4.46), 614sh (4.44) and 669 (4.04); δ_H(400 MHz; $CDCl_3$) −2.52 (2 H, s, inner NH), −2.44 (4 H, s, inner NH), 1.52–1.66 (216 H, m, *t*-butyl H), 4.43 (2 H, s, bridging H), 4.51 (2 H, d, J_{gem} 18.1, bridging H), 4.77 (2 H, d, J_{gem} 18.1, bridging H), 7.58–7.65 (4 H, m, quinoxalino H), 7.77–7.81 (4 H, m, aryl H and biquinoxalinyl H), 7.88–7.91 (4 H, m, aryl H), 7.95–8.25 (34 H, m, aryl H and biquinoxalinyl H), 8.77 (2 H, s, β-pyrrolic H), 8.80 (2 H, s, β-pyrrolic H), 8.83 (1 H, d, *J* 4.8, β-pyrrolic H), 8.87–8.89 (1 H, m, β-pyrrolic H), 8.94 (1 H, d, *J* 4.8, β-pyrrolic H), 8.97–9.03 (4 H, m, β-pyrrolic H) and 9.05–9.11 (5 H, m, β-pyrrolic H); *m/z* (MALDI-TOF) 3663.1 (M^+ requires 3663.2).

The second band observed during size exclusion chromatography was collected, the solvent removed under a vacuum and the residue recrystallised from a dichloromethane–methanol solution to yield extended Tröger's base bis-porphyrin **33** (65 mg, 44%) as brown crystals, mp >300 °C, which co-chromatographed and had an identical ^{1}H NMR spectrum to an authentic sample.[26]

Acknowledgements

This work was partially supported by a Discovery Research Grant (DP0208776) to M. J. C. from the Australian Research Council. Australian Post-graduate Research awards to P. J. S., and to J. A. H. are also gratefully acknowledged.

References

1 R. E. Blankenship, *Molecular Mechanisms of Photosynthesis*, Blackwell Science, Oxford, UK, 2002.
2 J. Deisenhofer and H. Michel, *Science*, 1989, **245**, 1463–147.
3 P. Jordan, P. Fromme, H.-T. Witt, O. Klukas, W. Saenger and N. Krauss, *Nature*, 2001, **411**, 909–917.
4 A. Zouni, H.-T. Witt, J. Kern, P. Fromme, N. Krauss, W. Saenger and P. Orth, *Nature*, 2001, **409**, 739–743.
5 M. J. Crossley and P. L. Burn, *J. Chem. Soc., Chem. Commun.*, 1991, 1569–1571.
6 H. L. Anderson, *Inorg. Chem.*, 1994, **33**, 972–981.
7 A. Tsuda and A. Osuka, *Science*, 2001, **293**, 79–82.
8 A. K. Burrell, D. L. Officer, P. G. Plieger and D. C. W. Reid, *Chem. Rev.*, 2001, **101**, 2751–2796.
9 J. T. Fletcher and M. J. Therien, *Inorg. Chem.*, 2002, **41**, 331–341.
10 M. J. Crossley, P. J. Sintic, R. Walton and J. R. Reimers, *Org. Biomol. Chem.*, 2003, **1**, 2777–2787.
11 E. K. L. Yeow, P. J. Sintic, N. M. Cabral, J. H. N. Reek, M. J. Crossley and K. P. Ghiggino, *Phys. Chem. Chem. Phys.*, 2000, **2**, 4281–4291.
12 J.-C. Chambron, V. Heitz and J.-P. Sauvage, in *Noncovalent Multiporphyrin Assemblies*, ed. K. M. Kadisk, K. M. Smith and R. Guilard, Academic Press, San Diego, CA, 2000, pp. 4–7.
13 J. L. Sessler, B. Wang, S. L. Springs and C. T. Brown, in *Electron- and Energy-transfer Reactions in Noncovalently Linked Supramolecular Model Systems*, ed. J. L. Atwood, J. E. D. Davies, D. D. MacNicol and F. Vögtle, Elsevier Science Ltd, Oxford, 1996, pp. 311–336.
14 H. Imahori, D. M. Guldi, K. Tamaki, Y. Yoshida, C. Luo, Y. Sakata and S. Fukuzumi, *J. Am. Chem. Soc.*, 2001, **123**, 6617–6628.
15 D. M. Guldi, *Chem. Soc. Rev.*, 2002, **31**, 22–36.
16 M. R. Wasielewski, *Chem. Rev.*, 1992, **92**, 435–461.
17 M.-J. Blanco, M. C. Jiménez, J.-C. Chambron, V. Heitz, M. Linke and J.-P. Sauvage, *Chem. Soc. Rev.*, 1999, **28**, 293–305.
18 I. M. Dixon, J.-P. Collin, J.-P. Sauvage, F. Barigelletti and L. Flamigni, *Angew. Chem., Int. Ed.*, 2000, **39**, 1292–1295.
19 M. Linke, J.-C. Chambron, V. Heitz, J.-P. Sauvage, S. Encinas, F. Barigelletti and L. Flamigni, *J. Am. Chem. Soc.*, 2000, **122**, 11834–11844.
20 J. R. Reimers, T. X. Lü, M. J. Crossley and N. S. Hush, *Chem. Phys. Lett.*, 1996, **256**, 353–359.
21 H. Imahori and Y. Sakata, *Eur. J. Org. Chem.*, 1999, 2445–2457.
22 D. Gust, T. A. Moore and A. L. Moore, *Acc. Chem. Res.*, 2001, **34**, 40–48.
23 D. Holten, D. F. Bocian and J. S. Lindsey, *Acc. Chem. Res.*, 2002, **35**, 57–69.
24 J. R. Reimers, N. S. Hush and M. J. Crossley, *J. Porphyrins Phthalocyanines*, 2002, **6**, 795–805.
25 D. H. Yoon, S. B. Lee, K.-H. Yoo, J. Kim, J. K. Lim, N. Aratani, A. Tsuda, A. Osuka and D. Kim, *J. Am. Chem. Soc.*, 2003, **125**, 11062–11064.
26 M. J. Crossley, A. C. Try and R. Walton, *Tetrahedron Lett.*, 1996, **37**, 6807–6114.
27 K. M. Kadish, W. E. Z. Ou, J. Shao, P. J. Sintic, K. Ohkubo, S. Fukuzumi and M. J. Crossley, *Chem. Commun.*, 2002, 356–357.
28 Z. Ou, K. M. Kadish, W. E. J. Shao, P. J. Sintic, K. Ohkubo, S. Fukuzumi and M. J. Crossley, *Inorg. Chem.*, 2004, **43**, 2078–2086.
29 S. Fukuzumi, K. Ohkubo, W. E. Z. Ou, J. Shao, K. M. Kadish, J. A. Hutchison, K. P. Ghiggino, P. J. Sintic and M. J. Crossley, *J. Am. Chem. Soc.*, 2003, **125**, 14984–14985.
30 *v. HYPERCHEM*, Hypercube Inc, Gainesville, FL, 2000.
31 M. J. Crossley and P. L. Burn, *J. Chem. Soc., Chem. Commun.*, 1987, 39–40.
32 M. J. Crossley, L. J. Govenlock and J. K. Prashar, *J. Chem. Soc., Chem. Commun.*, 1995, 2379–2380.
33 M. J. Crossley, P. L. Burn, S. J. Langford, S. M. Pyke and A. G. Stark, *J. Chem. Soc., Chem. Commun.*, 1991, 1567–1568.
34 A. Harriman, V. Heitz and J.-P. Sauvage, *J. Phys. Chem.*, 1993, **97**, 5940–5946.
35 N. Robertson and C. A. McGowan, *Chem. Soc. Rev.*, 2003, **32**, 96–103.
36 F. Barigelletti and L. Flamigni, *Chem. Soc. Rev.*, 2000, **29**, 1–12.
37 K. P. Ghiggino and T. A. Smith, *Prog. React. Kinet.*, 1993, **18**, 375–436.